Systematic profiling of a novel prognostic alternative splicing signature in hepatocellular carcinoma

DONG ZHANG[1,2], YI DUAN[1,2], ZHE WANG[3] and JIE LIN[4]

[1]Department of Breast Surgery, Qilu Hospital; [2]Clinical Medical College, Shandong University, Jinan, Shandong 250012; Departments of [3]Gastrointestinal Oncology and [4]General Surgery (VIP Ward), Cancer Hospital of China Medical University, Liaoning Cancer Hospital and Institute, Shenyang, Liaoning 110042, P.R. China

Abstract. Alternative splicing (AS) is a pervasive and vital mechanism involved in the progression of cancer by expanding genomic encoding capacity and increasing protein complexity. However, the systematic analysis of AS in hepatocellular carcinoma (HCC) is lacking and urgently required. In the present study, genome-wide AS events with corresponding clinical information were profiled in 290 patients with HCC from the Cancer Genome Atlas and SpliceSeq software. Functional enrichment analyses revealed the pivotal biological process of AS regulation. Univariate Cox regression analyses were performed, followed by stepwise forward multivariate analysis to develop the prognostic signatures. Spearman's correlation analyses were also used to construct potential regulatory network between the AS events and aberrant splicing factors. A total of 34,163 AS events were detected, among which 1,805 AS events from 1,314 parent genes were significantly associated with the overall survival (OS) of patients with HCC, and their parent genes serve crucial roles in HCC-related oncogenic processes, including the p53 signaling pathway, AMPK signaling pathway and HIF-1 signaling pathway. A prognostic AS signature was established that was found to be an independent prognostic factor for OS in stratified cohorts, harboring a noteworthy ability to distinguish between the distinct prognoses of patients with HCC (high-risk vs. low-risk, 827 vs. 3,125 days, P<2e-16). Time-dependent receiver-operator characteristic curves confirmed its robustness and clinical efficacy, with the area under the curves maintained >0.9 for short-term and long-term prognosis prediction. The splicing correlation network suggested a trend in the interactions between splicing factors and prognostic AS events, further revealing the underlying mechanism of AS in the oncogenesis of HCC. In conclusion, the present study provides a comprehensive portrait of global splicing alterations involved in the progression and HCC in addition to valuable prognostic factors for patients, which may represent as underappreciated hallmark and provide novel clues of therapeutic targets in HCC.

Correspondence to: Dr Jie Lin, Department of General Surgery (VIP Ward), Cancer Hospital of China Medical University, Liaoning Cancer Hospital and Institute, 44 Xiaoheyan Road, Dadong, Shenyang, Liaoning 110042, P.R. China
E-mail: linjie@cmu.edu.cn

Abbreviations: AA, alternate acceptor site; AD, alternate donor site; AFP, α-fetoprotein; AP, alternate promoter; AS, alternative splicing; AT, alternate terminator; AUC, area under the curve; BP, biological process; CC, cellular component; CI, confidence intervals; ES, exon skip; FDR, false discovery rate; GO, Gene Ontology; GSVA, gene set variation analysis; HCC, hepatocellular carcinoma; HR, hazard ratio; KEGG, Kyoto Encyclopedia of Genes and Genomes; ME, mutually exclusive exons; MF, molecular function; OS, overall survival; PSI, percent spliced in; RI, retained intron; ROC, receiver-operator characteristic; SF, splicing factor; TCGA, The Cancer Genome Atlas; VST, variance stabilizing transformation

Introduction

Despite advances in screening, diagnosis and curative treatment, hepatocellular carcinoma (HCC) remains a leading cause of cancer-associated morbidity and mortality worldwide (1). As a complex and heterogeneous disease, HCC carries different molecular profiles, distinct clinical responses to therapeutic agents and thus an unfavorable prognosis, with a mortality rate of ~500,000 worldwide per year (2,3). The recurrence rate is high, even for patients who have undergone curative resection with early-stage HCC, rendering the 5 year survival probability of <30% in patients suffered from HCC (4,5). Current risk assessment, treatment decisions and prognostic prediction of HCC mainly rely on features restricted to a cancer cell-centric focus, such as the tumor-node-metastasis (TNM) stage and Child-Pugh scoring system (6,7). However, conventional clinicopathological characteristics do not enable the precise predicting of individualized prognoses in patients with HCC. Such poor outcomes and high heterogeneity highlight challenging issues and the urgent need to develop novel predictive biomarkers with potential links to patient prognosis and therapeutics options.

Recent advances in high-throughput technologies have unexpectedly provided an opportunity to define the

genome-wide landscape of HCC, and contributed to the rapid development of molecular signatures for prognostic prediction and the further personalization and precision of treatment paradigms (8-10). With the pervasive application of microarray and next-generation sequencing technology, studies involving mutations, copy number variation, gene expression, non-coding RNA expression and immune infiltration have been performed to identify potential HCC-related loci in oncogenic pathways and interpret complex scenarios in the malignant progression of HCC (11-15). These studies, although with promising outcomes, have primarily focused on transcriptional levels and driver mutations, whereas the systematic analysis of variations in transcript architecture has received less attention.

Alternative splicing (AS), as a post-transcriptional modification process, holds the potential to generate varied isoforms and reprogram protein diversity among ~90% of human multi-exon genes (16). Therein, the selective inclusion or exclusion of specific exon regions from precursor mRNAs, followed by multiple permutations and combinations of spliced exons are taken together to produce mature mRNA (17). As the most important mechanism for expanding the coding capacity and increasing the proteome complexity, AS has been experimentally validated as having a decisive role in controlling growth and development (18,19). The evidence accumulated in previous decades has demonstrated that specific splicing variants may be involved in several hallmarks of carcinogenesis, including anti-apoptotic mechanisms, angiogenesis, immune evasion, epithelial-mesenchymal transition and metastasis, further emphasizing the significance of AS for determining clinical outcomes in cancer, particularly HCC (19-25). However, few studies have systematically investigated the AS landscape within the HCC microenvironment and its association with prognosis. Further comprehensive understanding of the shifts in the splicing pattern involved in the regulation of HCC may be a vital step in developing targeted therapy and helping to predict treatment response and patient prognosis.

By contrast, splicing factors (SFs), as the executor of splicing behaviors, function in alternative exon usage and splicing site selection by recognizing *cis*-regulatory elements within the alternative exons or flanking introns (26-28). Substantial evidence implicates somatic mutations and the differential expression of SFs as the dominant mechanism in the initial steps of mRNA splicing in normal and cancer cells (29,30). Notably, aberrant SFs can give rise to the oncogenic splicing isoforms that confer various advantages to cancer cells (31,32). As AS events and their clinical relevance in malignancies are only superficially understood, it is imperative to elucidate the intricate interwoven relationships between particular SFs and AS events, and the intrinsic regulatory mechanism in HCC.

The Cancer Genome Atlas (TCGA) project supplements abundant resources for the investigation of genome-wide AS patterns in cancer. In the present study, to elucidate the global portrait of aberrant AS events in HCC, the integrated splicing variant data of 290 patients with HCC and corresponding clinical information were profiled based on the TCGA database. In addition, prognostic signatures were constructed with high clinical efficacy. Further assessment of the splicing regulatory network between SFs and their potential targets may shed new light on the mechanisms of genetic variants in tumorigenesis and development.

Materials and methods

Data curation process. Third-level mRNA sequencing data and corresponding clinical information of the HCC cohort were obtained from TCGA data portal (http://tcga-data. nci.nih.gov/), containing 374 HCC tissues and 50 adjacent non-tumor tissues (33). To generate the AS profiles for each patient with HCC, SpliceSeq (version 2.1), a java application that unambiguously quantifies the inclusion level of each exon and splice junction, was used to evaluate the mRNA splicing patterns for the patients with HCC (34). A total of 290 patients who met the following criteria were included: i) A definite histological diagnosis of HCC; ii) patients were alive at least 30 days following initial pathological diagnosis; iii) patients had corresponding mRNA splicing data. The percent spliced in (PSI) score, ranging from zero to one, was commonly used to evaluate the transcript ratio of a specific gene to a particular splicing pattern. In order to generate the most reliable set of AS events possible, a series of stringent filters were implemented (percentage of samples with PSI score ≥75 and average PSI score ≥0.05) and missing PSI values were input using the k-nearest neighbor algorithm with the impute R package (35).

To describe an AS event precisely, each AS event was assigned a unique annotation, which consisted of the particular splicing type, the ID number in the TCGASpliceSeq database and the matched gene symbol. For example, in 'RI_C9orf9_ ID_87994', the retained intron (RI) represents the splicing type, C9orf9 is the counterpart gene symbol and ID_87994 represents the specific order number in the TCGASpliceSeq database.

Survival analysis and construction of a prognostic signature for patients with HCC. Following rigorous screening, a total of 290 patients with HCC with aberrant AS profiles and survival information were subjected to subsequent analyses. For each specific AS event, the PSI scores were dichotomized based on the median cut among patients with HCC. Univariate Cox regression analyses were then performed to identify the association between AS events and overall survival (OS), with a threshold of P<0.05. UpSet plot, generated using the UpSetR R package (version 1.3.2; https://github.com/hms-dbmi/UpSetR), was used to qualitatively visualize the intersecting sets among seven types of survival-associated AS event (36). For high-dimension data, the traditional Cox regression model cannot be applied directly. To further reduce redundancy and render the model more practical and parsimonious, forward stepwise selection with the Akaike Information Criterion (AIC) was used, which starts with a null model and gradually adds the variable whose inclusion offers the most statistically significant improvement to the fitness of the model until balancing the AIC score of the model to a minimum (37). Therefore, among the top 20 (if available) most significant AS events within each AS type in univariate Cox regression analysis, the key AS events were sub-selected by the forward stepwise procedure to construct the AS signature, respectively. The AS events included in each AS signature were then combined to construct the final AS signature through a secondary implementation of forward stepwise selection. Finally, the AS-related risk score of each signature was calculated utilizing the regression coefficients derived from

multivariate Cox regression analysis to multiply the PSI score of each key feature, respectively. Based on the median cut-off value of the risk score, the log-rank test and Kaplan-Meier survival analysis were used to validate the statistical difference between the low-risk and high-risk subgroups. Furthermore, the clinical predictive efficacy of each prognostic signature was quantitatively evaluated by fitting the time-dependent receiver-operator characteristic (ROC) curve with the area under the curve (AUC) calculated. Therein, the model selection by AIC in a stepwise algorithm was based on the stepAIC function in the MASS R package, whereas the dynamic AUC values of the time-dependent ROC curve were calculated with the timeROC R package (38).

Independence of the final AS signature from clinicopathological features. To investigate the independent prognostic value of the final AS signature from the available conventional clinicopathological characteristics (including age, gender, alcohol consumption history, hepatitis B status, hepatitis C status, family cancer history, serum α-fetoprotein (AFP) level, Child-Pugh classification, residual tumor status, vascular invasion degree, histologic grade and pathologic stage) in patients with HCC, univariate and subsequent multivariate Cox regression analyses were performed. To confirm whether the final AS signature was of high applicability and robust in various subgroups, stratification Cox analyses were also conducted.

Functional enrichment and interaction analysis of survival-associated AS events. The parent genes of the survival-associated AS events determined by univariate Cox regression analysis were subjected to Gene Ontology (GO) and Kyoto Encyclopedia of Genes and Genomes (KEGG) pathway analyses by setting the false discovery rate (FDR) <0.05. The above analyses were performed with clusterProfiler R package (version 3.7) (39). Additionally, the gene interaction network was visualized and analyzed using the Reactome FIPlugIn (version 7.0.2; http://apps.cytoscape.org/apps/reactomefiplugin) in Cytoscape (version 3.6.1) with the purpose of searching important hub genes.

Construction of the potential SF-AS regulatory network in the HCC cohort. A list of 88 human SFs was created by integrating the SpliceAid 2 database (www.introni.it/spliceaid.html) and the data reported by Xiong *et al*, who collected experimentally validated SFs through hand-curated screening of literature and databases (40). First, the corresponding expression levels of SFs in the TCGA-HCC dataset were integrated and normalized with the variance stabilizing transformation function of the DESeq2 package (41,42). The HCC samples and adjacent normal samples were compared to identify differentially expressed SFs using Student's t-test. The correlation between the normalized expression value of SFs and OS was then assessed through fitting univariate regression analysis in the entire cohort, for which SFs with P<0.05 were selected as prognostic SFs for further analysis. The 'surv_cutpoint' function of the 'survminer' R package was used to iteratively determine the optimal cutpoints of prognostic SFs achieving the maximally selected rank statistics. Furthermore, Spearman's correlation analyses were performed between the expression values of prognostic SFs and PSI scores of the most significant AS events in each AS type. P-values were adjusted by the

Benjamini-Hochberg procedure and the significance threshold was set at adjusted P<0.05.

Gene set variation analysis (GSVA) for SF-AS correlation pairs. GSVA is a differential functional gene set enrichment analysis, which can detect subtle pathway activity changes over heterogeneous samples by calculating sample-wise gene set enrichment scores. GSVA was performed using the GSVA package from Bioconductor (release version 3.8; www.bioconductor.org) to further search for a significantly enriched set of GO and canonical pathways (KEGG, Reactome and BioCarta pathway databases) in HCC tissues, downloaded from the Molecular Signatures Database (www.broadinstitute.org) (43). Differential gene set analysis between the tumor and adjacent normal samples was then performed using the limma package (44). |logFC| >0.4 and FDR <0.05 for GO terms and |logFC| >0.2 and FDR <0.05 for pathway sets were considered statistically significant, respectively.

Results

Overview of AS events in the TCGA HCC cohort. The integrated mRNA sequencing data of 290 patients with HCC with AS events profiles were included in the present study. The median follow-up period was 15.75 months (range 1-122.5 months). Details of the study design are presented as a flowchart in Fig. 1A. Overall, a total of 34,163 AS events from 8,986 parent genes were detected based on the results of SpliceSeq analysis. As shown in Fig. 1C, seven types of AS event were generated via different mechanisms. Furthermore, the AS events and genes in each AS type were separated into a survival-related group (P<0.05) or a survival-irrelevant group (P≥0.05) (Fig. 1B). In total, 1,805 survival-associated AS events were identified from 1,314 parent genes, which contained 565 exon skips (ESs) in 479 genes, 541 alternate terminators (ATs) in 356 genes, 341 alternate promoters (APs) in 258 genes, 137 alternate acceptor sites (AAs) in 128 genes, 112 RIs in 104 genes, 100 alternate donor sites (ADs) in 95 genes and nine mutually exclusive exons (MEs) in nine genes. It was noted that one gene may have two or more AS events associated with OS, therefore, an UpSet plot was generated to quantitatively analyze the interactive sets between the seven AS types (Fig. 1D). Accordingly, the survival-associated AS events mostly belonged to one parent gene, whereas several genes had up to four types of AS event which were all significantly related to prognosis. For example, RI, AA, AP and ES in the CIRBP gene (red dotted line) were significantly associated with OS in HCC, and AD, AP and ES in the BSCL2 gene (green dotted line) were significantly associated with OS in HCC.

Survival analysis and construction of a prognostic signature for patients with HCC. To identify independent prognostic factors, univariate Cox survival analysis was performed to assess the association between clinical OS and each type of AS event. In each AS event, the patients with HCC were divided into two subgroups based on the median PSI score. The top 20 significant survival-associated events of the seven types of AS, with the exception of ME with only nine AS events, are presented as forest plots in Fig. 2. As shown in the
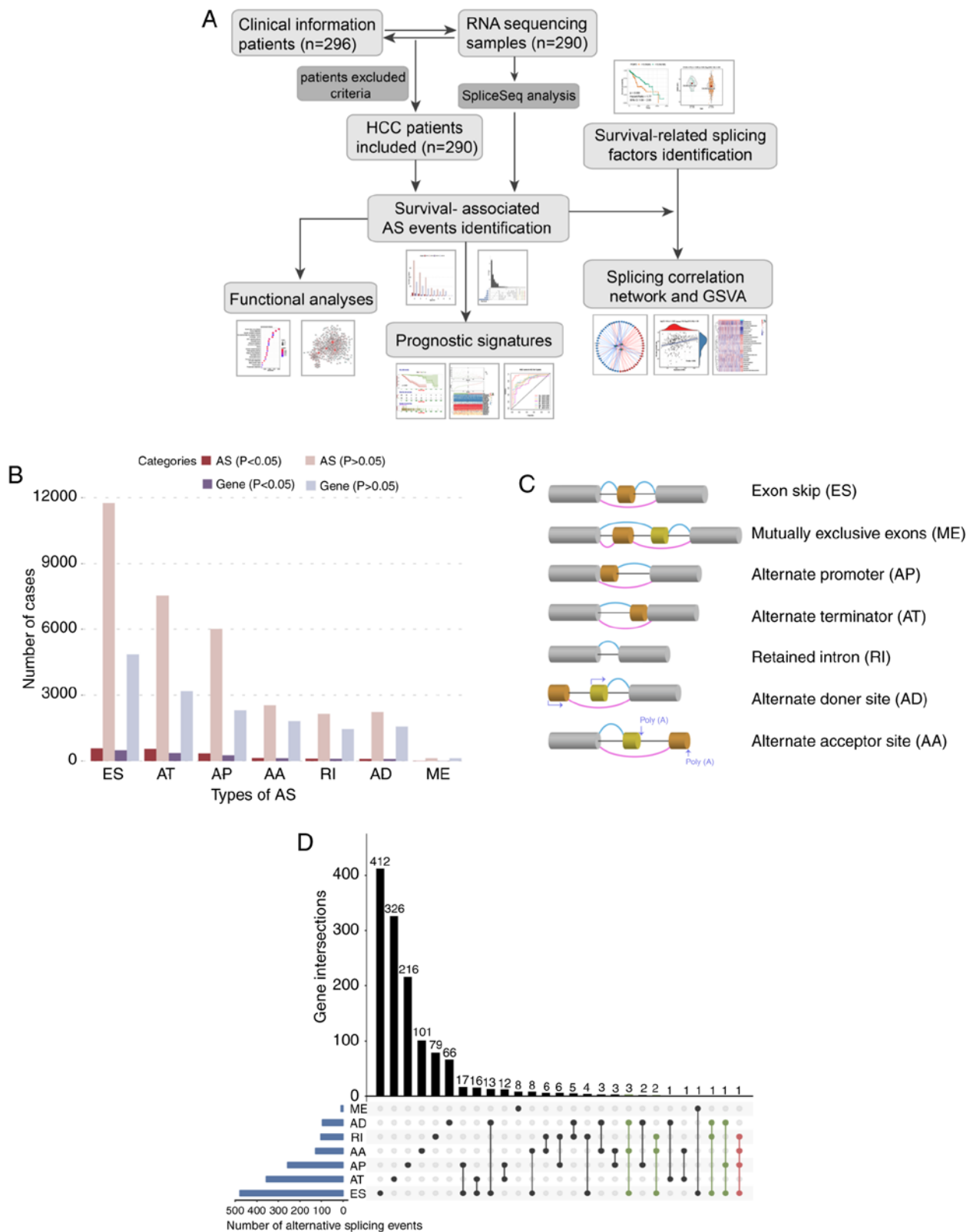
Figure 1. Overview of AS events profiling in HCC. (A) Flowchart for profiling the AS events of patients with HCC in large-scale sequencing data. (B) Number of AS events and parent genes from 290 patients with HCC. (C) Illustrations for seven types of AS events, including ES, ME, RI, AP, AT, AD and AA. (D) UpSet plot of parent gene interactions between the seven types of survival-associated AS events in HCC. AS, alternative splicing; HCC, hepatocellular carcinoma; GSVA, gene set variation analysis; ES, exon skip; ME, mutually exclusive exons; RI, retained intron; AP, alternate promoter; AT, alternate terminator; AD, alternate donor site; AA, alternate acceptor site.

forest plots, it appeared that the survival-associated AS events were almost equally distributed in the favorable prognostic and reverse subgroups, regardless of the AS type. Notably,

AS signatures constructed with 11 ES events, six AT events, 10 AD events, 10 AA events, seven AP events, six RI events or seven ME events all showed significant predictive power in
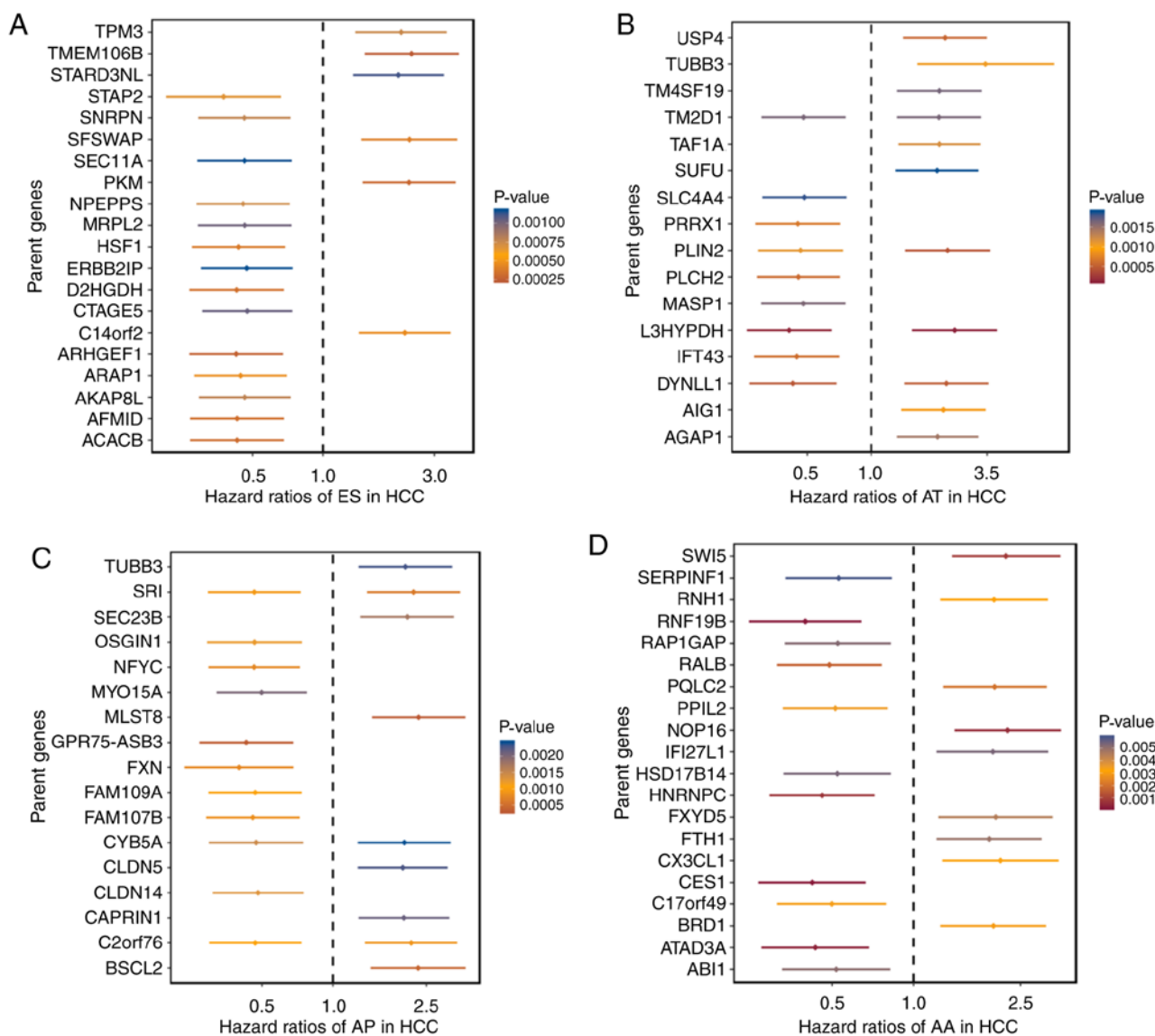
Figure 2. Forrest plots of hazard ratios of survival-associated alternative splicing events in HCC. Hazard ratios of top 20 most significant survival-associated (A) ES, (B) AT, (C) AP, (D) AA. P-values are indicated by the color scale of the legend. HCC, hepatocellular carcinoma; ES, exon skip; AT, alternate terminator; AP, alternate promoter; AA, alternate acceptor site; RI, retained intron; AD, alternate donor site; ME, mutually exclusive exons.

distinguishing poor or good clinical outcomes for the patients with HCC (P<0.0001), and AA, AP, AT and ES had the highest predictive power among the seven types with a median survival of >3,000 days in the low-risk subgroup (Fig. 3A-G). A final prognostic model, which included only 26 AS events to minimize the AIC, was then constructed (high vs. low: 827 vs. 3,125 days, P<2e-16, Fig. 5A). Furthermore, the ROC curves of 1, 3 and 5 years were applied to compare the predictive efficiency among different AS models. As shown in Fig. 5C, it was confirmed that the final prognostic model incorporated with all types of AS event exhibited a higher prognostic efficiency compared with the others, and the AUCs for 1, 3 and 5 years were 0.937, 0.902 and 0.985, respectively. Additionally, the distribution of the survival status and risk scores of patients, and the splicing pattern of specific AS events included in each signature were visualized (Figs. 4 and 5B). Detailed information of the specific AS events involved in each AS signature and final prognostic model are listed in Table I. Additionally, the relative PSI scores of particular AS events comprised in

the final AS signature between the low-risk and high-risk subgroups are depicted in Fig. S1.

Independent predictive power of the final AS signature for patients with HCC. Univariate and multivariate Cox hazard regression analyses of data in the TCGA HCC cohort were performed in order to further investigate whether the final AS-based signature was an independent prognostic factor, with the AS signature treated as a binary variable. The results of comprehensive univariate analysis suggested that age, hepatitis B status, family cancer history, serum AFP level, degree of vascular invasion, pathologic stage and AS signature were all correlated with the OS of patients with HCC (Fig. 6A). Therefore, these significant risk factors were included in a multivariate analysis, which showed that the AS signature (HR: 12.573; 95% CI: 4.957-31.893; P=9.79e-08), AFP level and vascular invasion were three independent prognostic factors when adjusted by those factors (Fig. 6B). In addition, in order to investigate the prognostic value of the AS signature
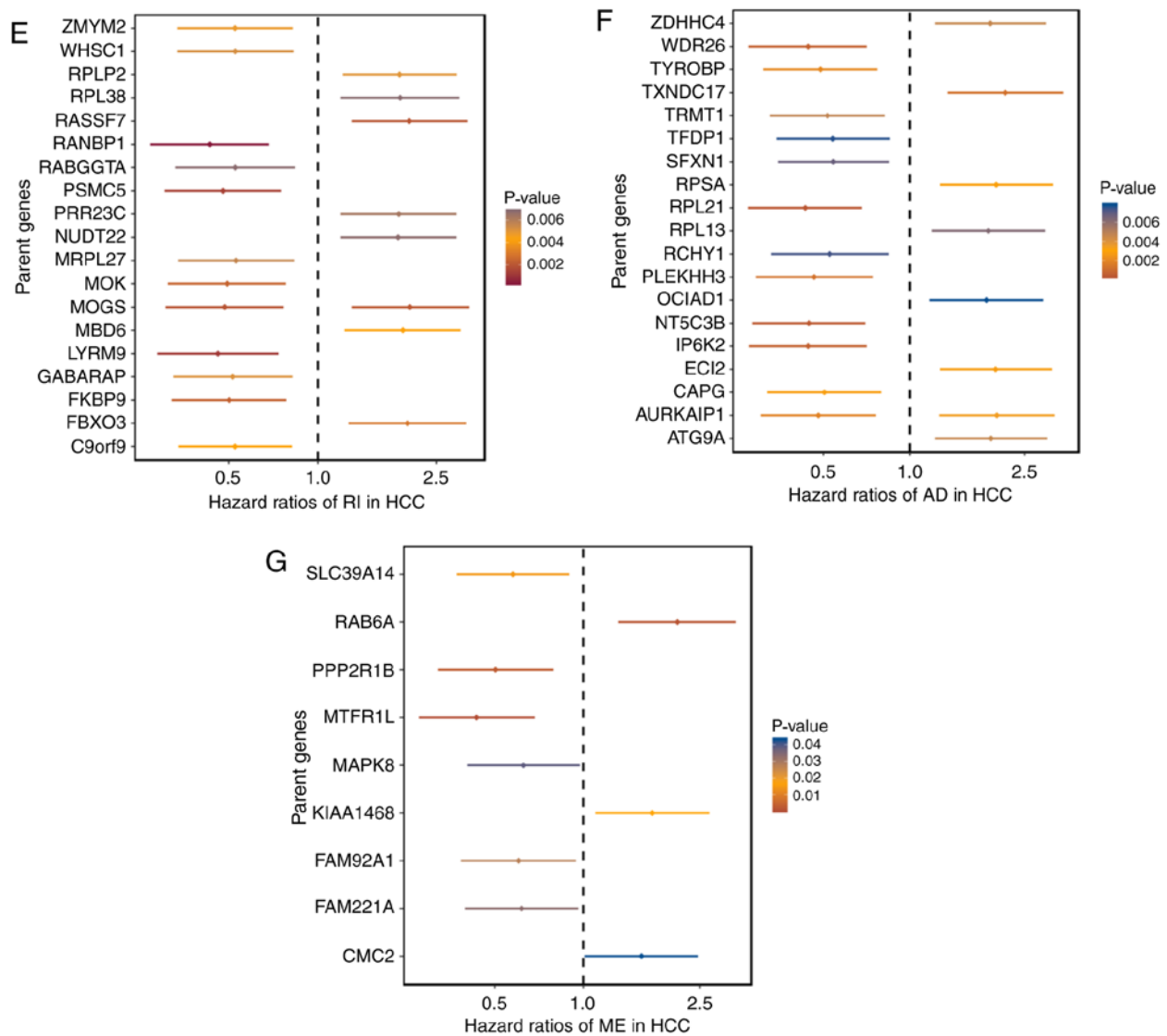
Figure 2. Continued. Forrest plots of hazard ratios of survival-associated alternative splicing events in HCC. Hazard ratios of top 20 most significant survival-associated (E) RI and (F) AD events. (G) Hazard ratios of significant survival-associated ME events (only nine available). P-values are indicated by the color scale of the legend. HCC, hepatocellular carcinoma; ES, exon skip; AT, alternate terminator; AP, alternate promoter; AA, alternate acceptor site; RI, retained intron; AD, alternate donor site; ME, mutually exclusive exons.

in a stratified cohort, the patients were classified into various subgroups based on relative complete clinical features and stratification analysis was performed. As shown in Fig. S2, the prognostic signature identified patients with distinct prognoses in all cohorts analyzed, thus confirming its robustness for independently predicting HCC prognosis.

Functional enrichment and interaction analysis of survival-associated AS events. To shed light on the potential impact of prognostic AS events to their corresponding proteins, GO and KEGG enrichment analyses were conducted based on those parent genes that generated prognostic AS events. A total of 20 GO terms were identified in the aspect of molecular function (MF), including cell adhesion molecule binding and cadherin binding pathways (Fig. 7B). A total of 176 biological process (BP) terms (Fig. 7C) and 71 cellular component (CC) terms (Fig. 7D) were also enriched significantly, indicating obvious changes in the purine-related metabolic process, protein targeting, focal adhesion and cell-surface junction pathways.

Additionally, the KEGG enrichment analysis revealed a total of 48 enriched pathways, the majority of which were relevant to the liver cancer trilogy, invasiveness and distant metastasis of hepatoma cells, cancer pathway and nucleotide metabolism (Fig. 7E). Of note, certain KEGG pathways that are known to be involved in tumorigenesis and the progression of HCC were also enriched, including ubiquitin-mediated proteolysis (FDR <0.0067), p53 signaling pathway (FDR <0.028), AMPK signaling pathway (FDR <0.017), HIF-1 signaling pathway (FDR <0.0059) and EGFR tyrosine kinase inhibitor resistance (FDR <0.017). Coincidentally, cancer-related pathways were also identified, including colorectal cancer, glioma, pancreatic cancer, endometrial cancer and non-small cell lung cancer (Fig. 7E). Taken together, the parent genes associated with prognostic AS events may serve an important role in the carcinogenesis, progression and metastasis of HCC. Therefore, these specific dysregulated AS events may orchestrate the post-transcriptional modification of parent genes and further modify protein features in patients with
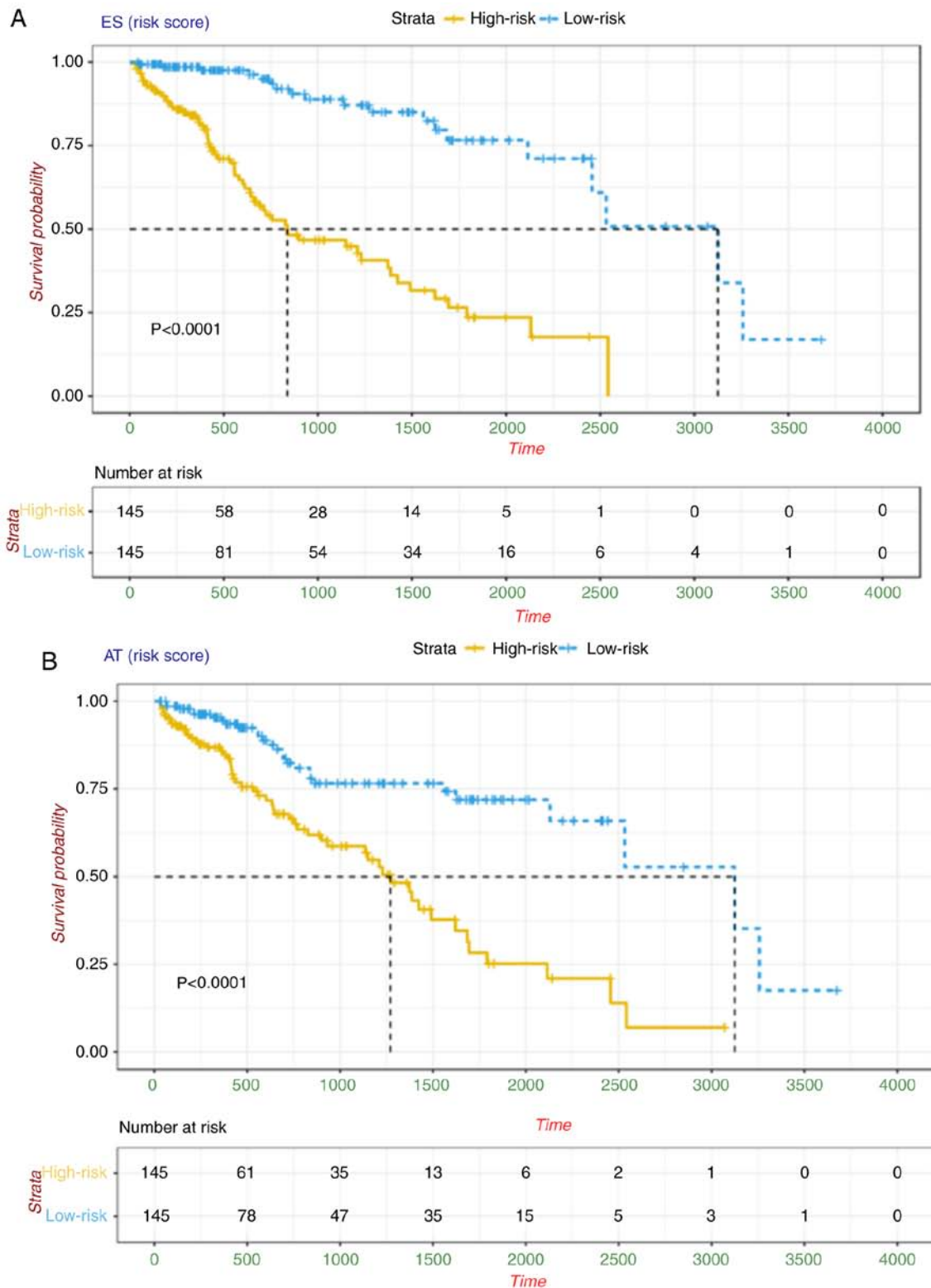
Figure 3. Kaplan-Meier plots of AS signatures built with seven types of AS events in HCC. Kaplan-Meier curves of prognostic predictors built with candidate (A) ES and (B) AT. The yellow line indicates the high-risk subgroup and the blue line indicates the low-risk subgroup. P-values and median survival times (dotted line) are shown in each signature. HCC, hepatocellular carcinoma; AS, alternative splicing; ES, exon skip; AT, alternate terminator; AP, alternate promoter; AA, alternate acceptor site; RI, retained intron; AD, alternate donor site; ME, mutually exclusive exons.

HCC. Furthermore, to demonstrate the interactive relationship between the prognostic AS events from a biological systems point of view, all of the identified parent genes in HCC were input into Cytoscape to generate a gene interaction network. The results revealed several important hub genes

in the entire network, including TP53, EGFR, HSPA8 and UPF3B (Fig. 7A).

Potential cancer-specific SF-AS regulatory network in the HCC cohort. It has been shown that the global
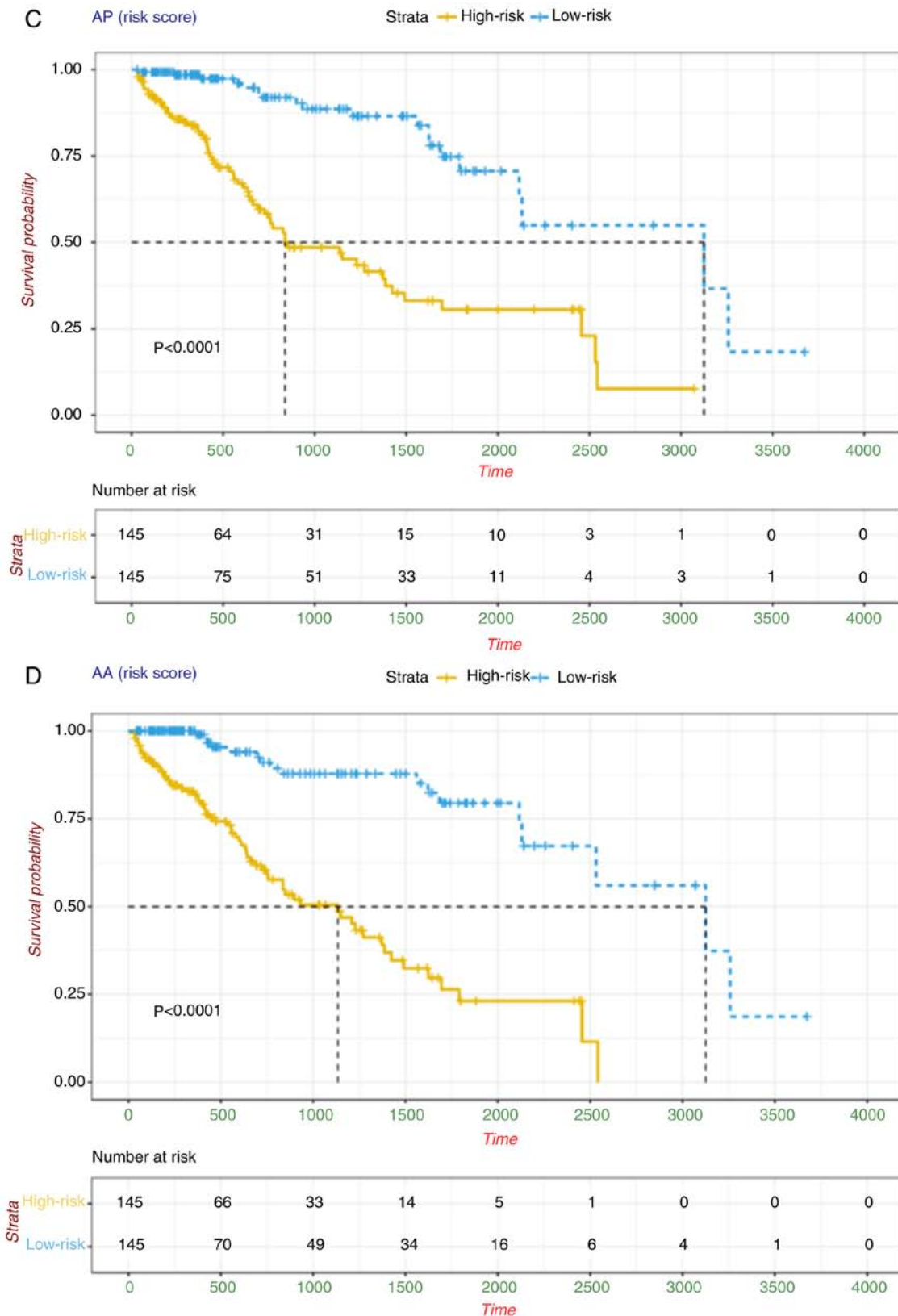
Figure 3. Continued. Kaplan-Meier plots of AS signatures built with seven types of AS events in HCC. Kaplan-Meier curves of prognostic predictors built with candidate (C) AP and (D) AA. The yellow line indicates the high-risk subgroup and the blue line indicates the low-risk subgroup. P-values and median survival times (dotted line) are shown in each signature. HCC, hepatocellular carcinoma; AS, alternative splicing; ES, exon skip; AT, alternate terminator; AP, alternate promoter; AA, alternate acceptor site; RI, retained intron; AD, alternate donor site; ME, mutually exclusive exons.

prognosis-related AS events can be orchestrated by a limited number of SFs, particularly in HCC. With access to normalized level-three RNA-seq profiles of TCGA-HCC samples, the present study identified 53 SFs whose expression levels differed significantly between tumor tissues and adjacent normal tissues, among which 27 SFs were upregulated and 26
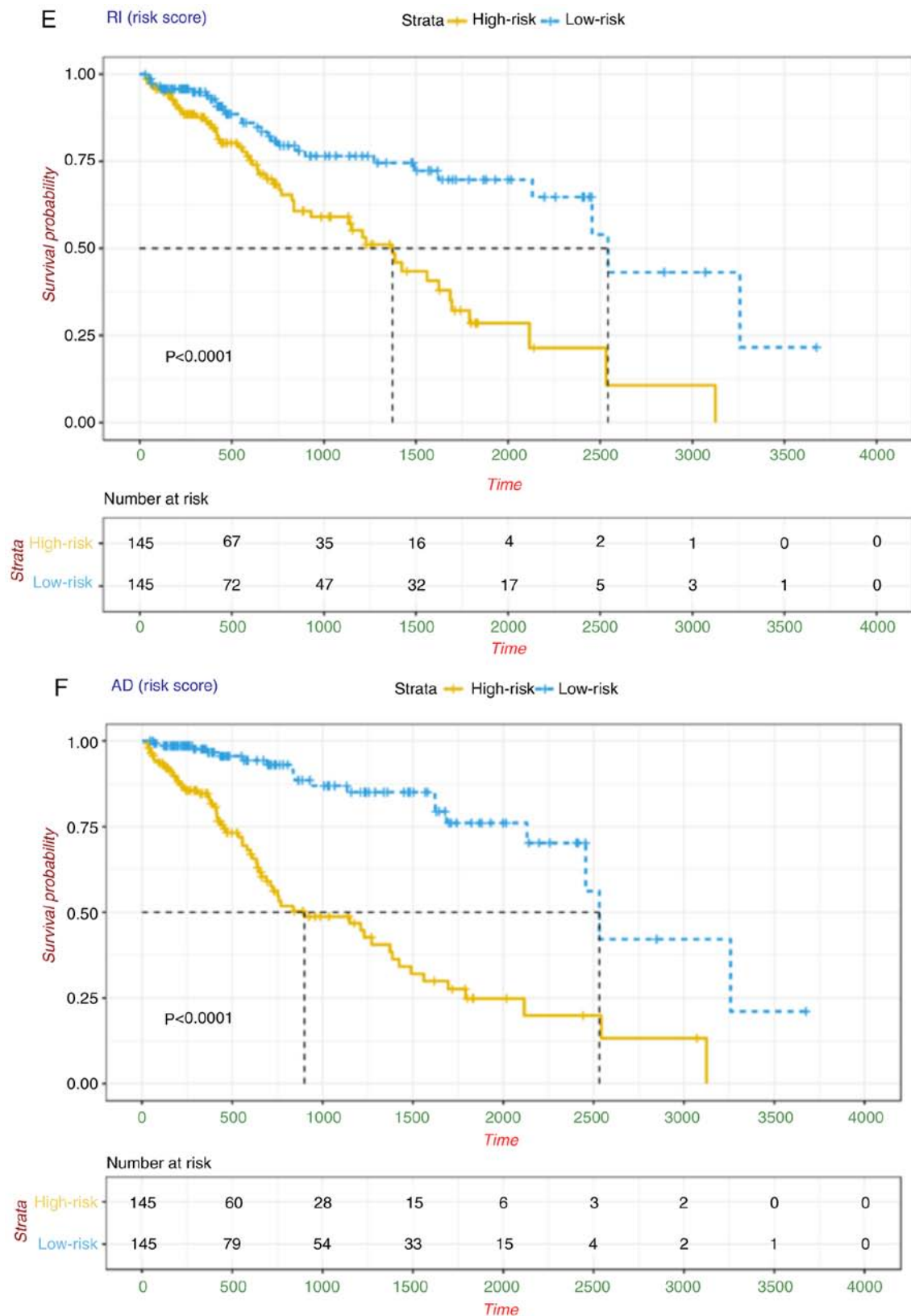
Figure 3. Continued. Kaplan-Meier plots of AS signatures built with seven types of AS events in HCC. Kaplan-Meier curves of prognostic predictors built with candidate (E) RI and (F) AD. The yellow line indicates the high-risk subgroup and the blue line indicates the low-risk subgroup. P-values and median survival times (dotted line) are shown in each signature. HCC, hepatocellular carcinoma; AS, alternative splicing; ES, exon skip; AT, alternate terminator; AP, alternate promoter; AA, alternate acceptor site; RI, retained intron; AD, alternate donor site; ME, mutually exclusive exons.

were downregulated (Fig. 8A). To systematically analyze the cancer-specific splicing regulatory connections between SFs and AS events in HCC, the prognostic SFs were identified and a cancer-specific SF-AS correlation network was constructed. In this network, three SFs, including PCBP2 (P=0.009, HR: 1.77, 95% CI: 1.09-2.85), SFPQ (P<0.001, HR: 2.02,
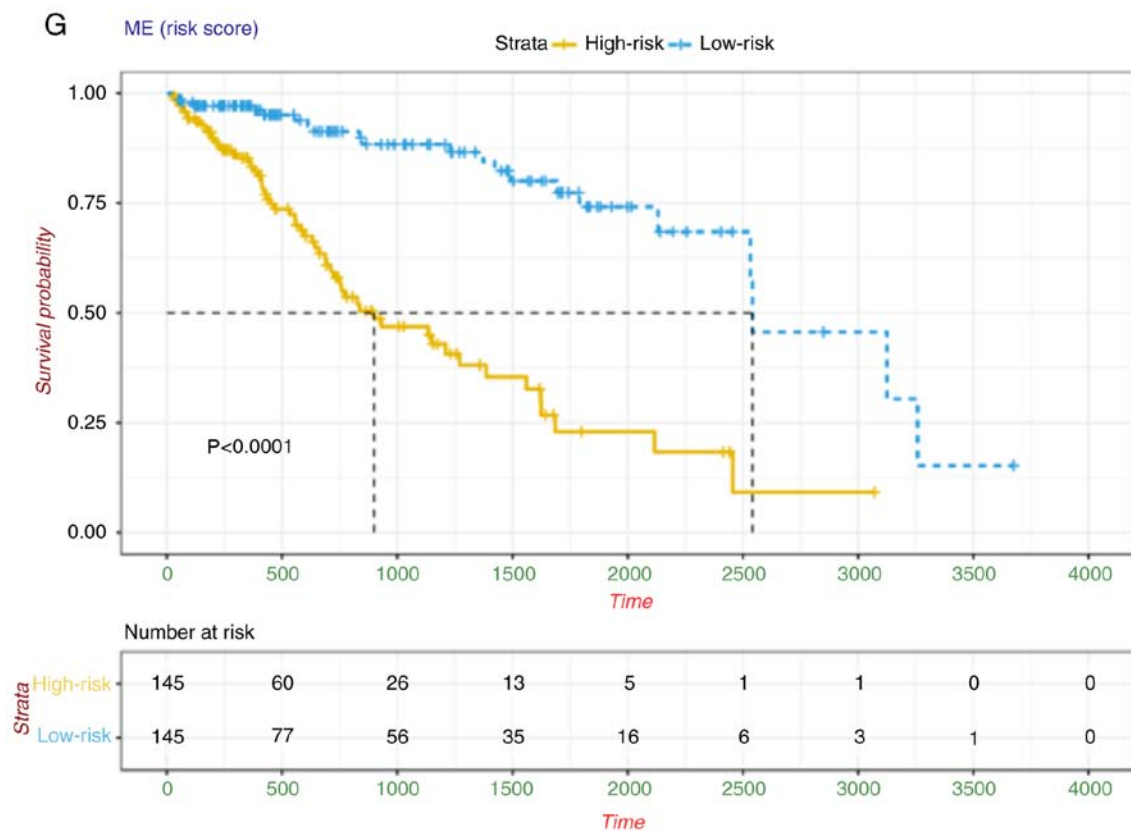
Figure 3. Continued. Kaplan-Meier plots of AS signatures built with seven types of AS events in HCC. Kaplan-Meier curves of prognostic predictors built with candidate (G) ME events in HCC, respectively. The yellow line indicates the high-risk subgroup and the blue line indicates the low-risk subgroup. P-values and median survival times (dotted line) are shown in each signature. HCC, hepatocellular carcinoma; AS, alternative splicing; ES, exon skip; AT, alternate terminator; AP, alternate promoter; AA, alternate acceptor site; RI, retained intron; AD, alternate donor site; ME, mutually exclusive exons.

95% CI: 1.25-3.27) and SRSF10 (P=0.019, HR: 1.74, 95% CI: 1.12-2.7) were screened as being prognostic (Fig. 8C), and their corresponding expression levels are presented in Fig. 8B. In addition, a total of 62 survival-associated AS events were used for constructing an SF-AS regulatory network (Fig. 8D), among which were 26 risky AS events (HR >1) and 36 favorable events (HR <1). Of note, the majority of risky prognostic AS events (red dots) were positively correlated (red lines) with the expression of SFs (green diamonds), whereas favorable prognostic AS events (blue dots) were negatively correlated (blue lines) with these SFs. It appears that aberrant AS events can be co-regulated by the synergistic or competitive influence of distinct prognostic SFs. These results further demonstrated the underlying mechanisms that indicate AS offer potential in expanding the coding capacity of transcripts. In addition, representative correlation pairs within this regulatory network are shown in scatter plots (Fig. 8E). For example, the expression of SFPQ was positively correlated with the RI event of RASSF7 but negatively correlated with the ES event of AFMID.

GSVA for SF-AS correlation pairs. The potential mechanism underlying the SF-AS regulatory relationships, either in a positive or negative correlation, was investigated. Spearman's correlation analyses were conducted between the identified SFs described above and survival-associated AS events, P-values were adjusted using the Benjamini-Hochberg correction. The significant SF-AS correlation pairs were filtered with an adjusted P-value of <0.05. The parent genes of these correlation pairs were then sent for GSVA and differential enrichment analysis between tumor and adjacent normal samples. The results were visualized as volcano plots and heatmaps, respectively (Figs. S3 and S4), which showed that the tumor tissue exhibited increased activities in cell proliferation and cell cycle, and decreased activities in immune response and cell adhesion.

Discussion

HCC is heterogeneous tumor from a molecular point of view (45). Over the last decade, significant efforts have been made to reveal the molecular changes in genomic profiles involved in the development of HCC (46). Such studies have contributed to the determination of prognostic genetic signatures, including genes, microRNAs and non-coding RNAs, which has promoted the identification of relevant prognostic markers and even therapeutic targets (47-49). In addition, as a major post-transcriptional biological behavior to expand genomic coding capacity and increase protein diversity, AS has been shown to have more potential significance in cancer biology.

Preliminary investigations of AS in HCC have demonstrated the crucial cancer-associated phenotypes can be converted by specific AS events and changes through inducing cell proliferation, promoting angiogenesis or avoiding apoptosis (20). For example, PKM2, resulting from ME events of exons 9 and 10 of the Pkm gene, is closely linked to the tumorigenesis of HCC by controlling cancer metabolic homeostasis
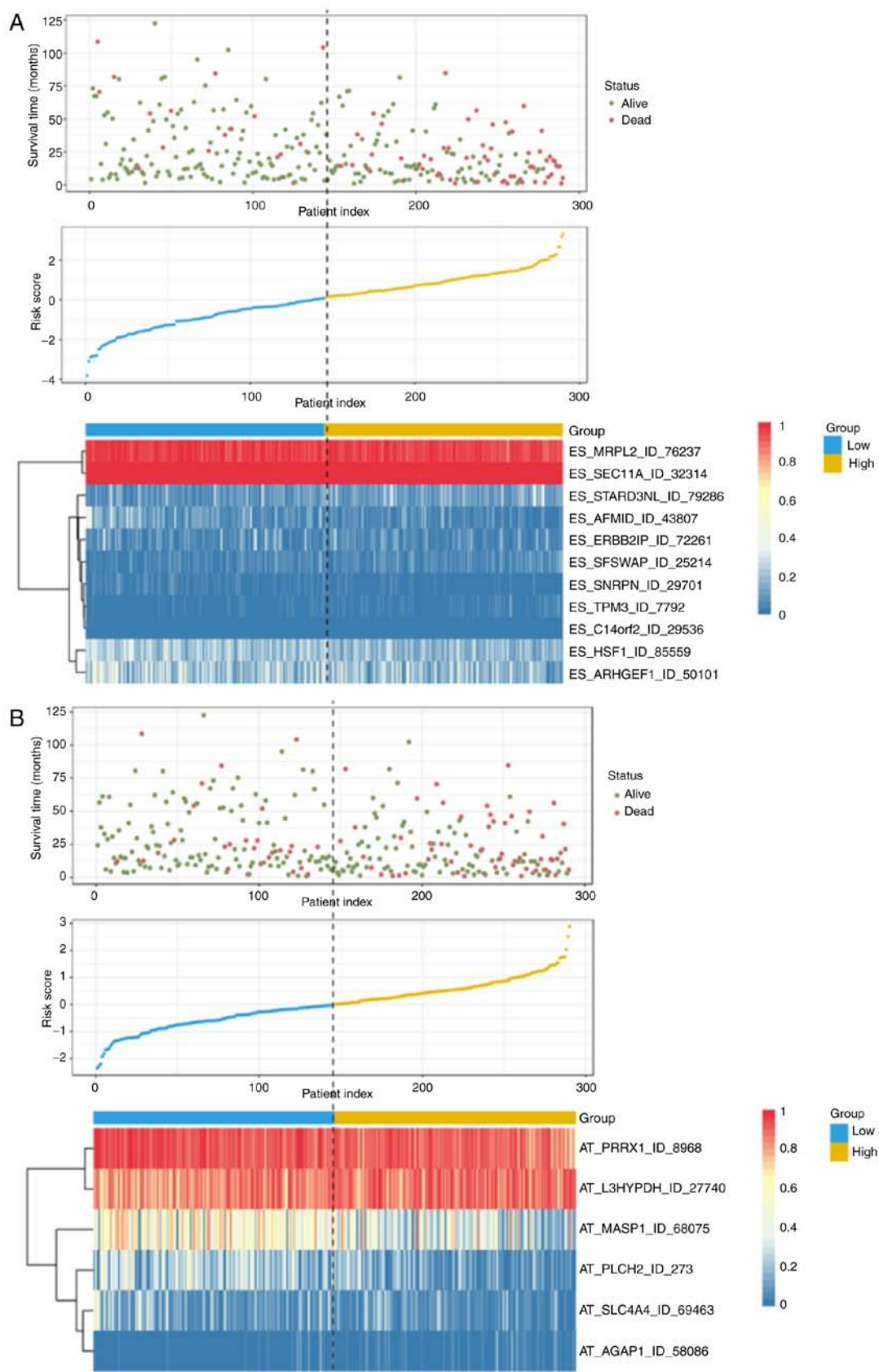
Figure 4. Determination and analysis of prognostic signatures based on each AS type in the HCC cohort. Distribution of the survival status and risk scores of patients, and the splicing pattern of AS events included in each AS signature are shown. Patients with HCC were divided into high- and low-risk subgroups based on the median cut-off risk score calculated separately. The upper part of each assembly indicates the distribution of the survival status and survival times of patients ranked by risk score, the middle part represents the risk score curve, and the heatmap below displays splicing pattern of the AS signature from each AS type. The color transition from blue to red indicates the increasing percent spliced in score of the corresponding AS event from low to high. For (A) ES and (B) AT risk scores (corresponding to each AS type) were calculated and AS signatures were constructed using each type of prognostic splicing event. HCC, hepatocellular carcinoma; AS, alternative splicing; ES, exon skip; AT, alternate terminator; AP, alternate promoter; AA, alternate acceptor site; RI, retained intron; AD, alternate donor site; ME, mutually exclusive exons.

Figure 4. Continued. The color transition from blue to red indicates the increasing percent spliced in score of the corresponding AS event from low to high. For (C) AP and (D) AA, risk scores (corresponding to each AS type) were calculated and AS signatures were constructed using each type of prognostic splicing event. HCC, hepatocellular carcinoma; AS, alternative splicing; ES, exon skip; AT, alternate terminator; AP, alternate promoter; AA, alternate acceptor site; RI, retained intron; AD, alternate donor site; ME, mutually exclusive exons.
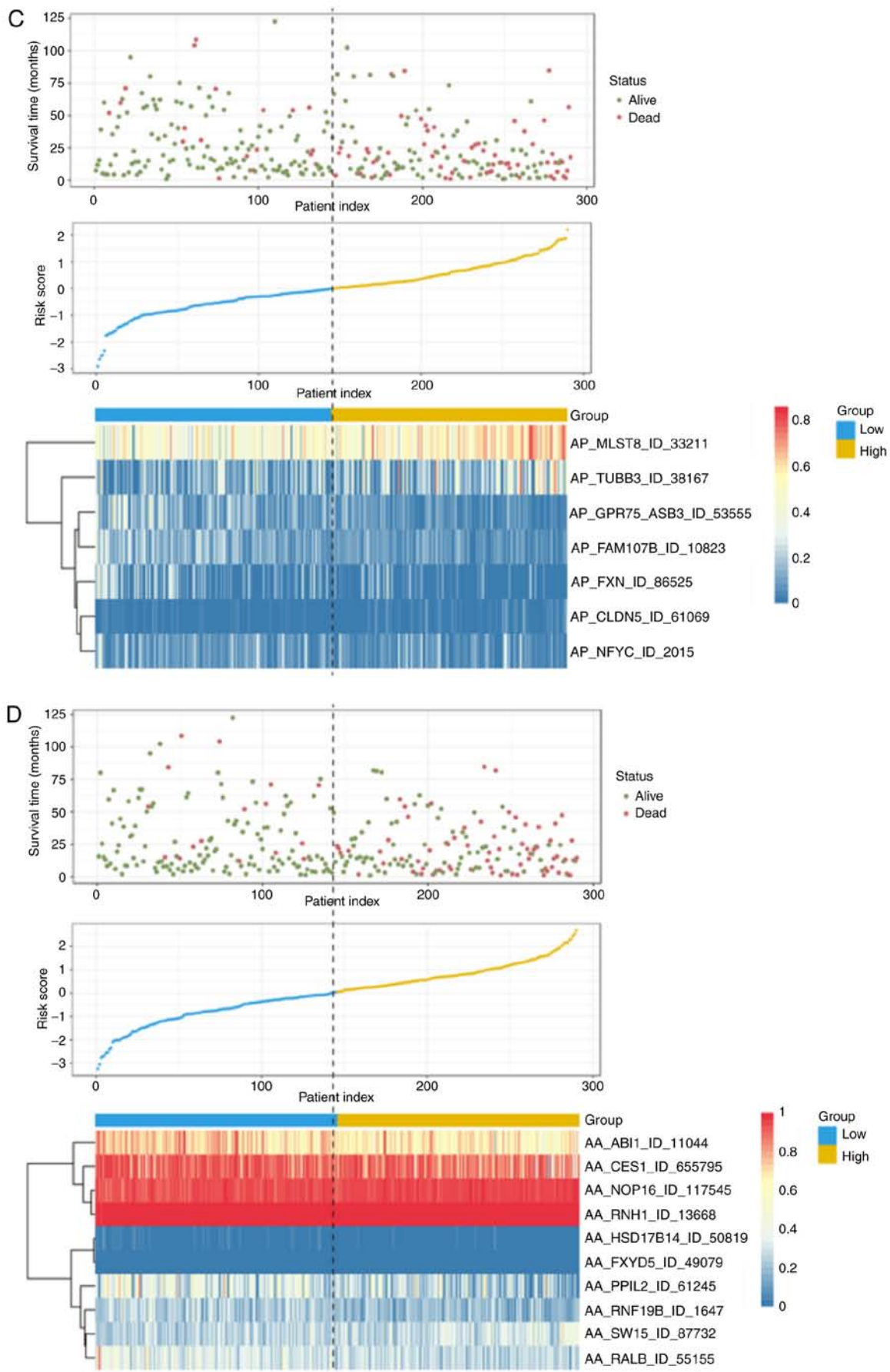
Figure 4. Continued. The color transition from blue to red indicates the increasing percent spliced in score of the corresponding AS event from low to high. For (E) RI and (F) AD risk scores (corresponding to each AS type) were calculated and AS signatures were constructed using each type of prognostic splicing event. HCC, hepatocellular carcinoma; AS, alternative splicing; ES, exon skip; AT, alternate terminator; AP, alternate promoter; AA, alternate acceptor site; RI, retained intron; AD, alternate donor site; ME, mutually exclusive exons.
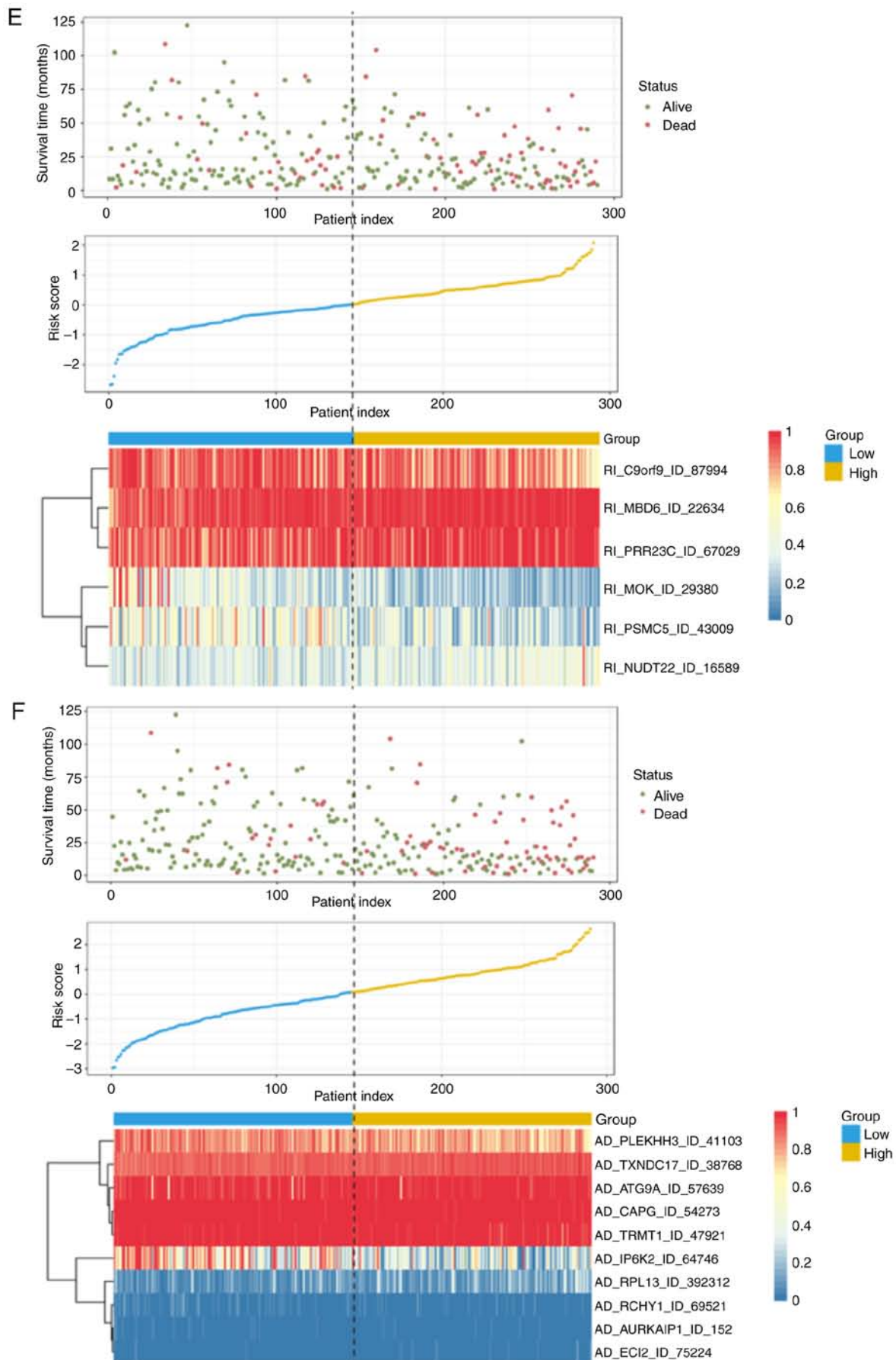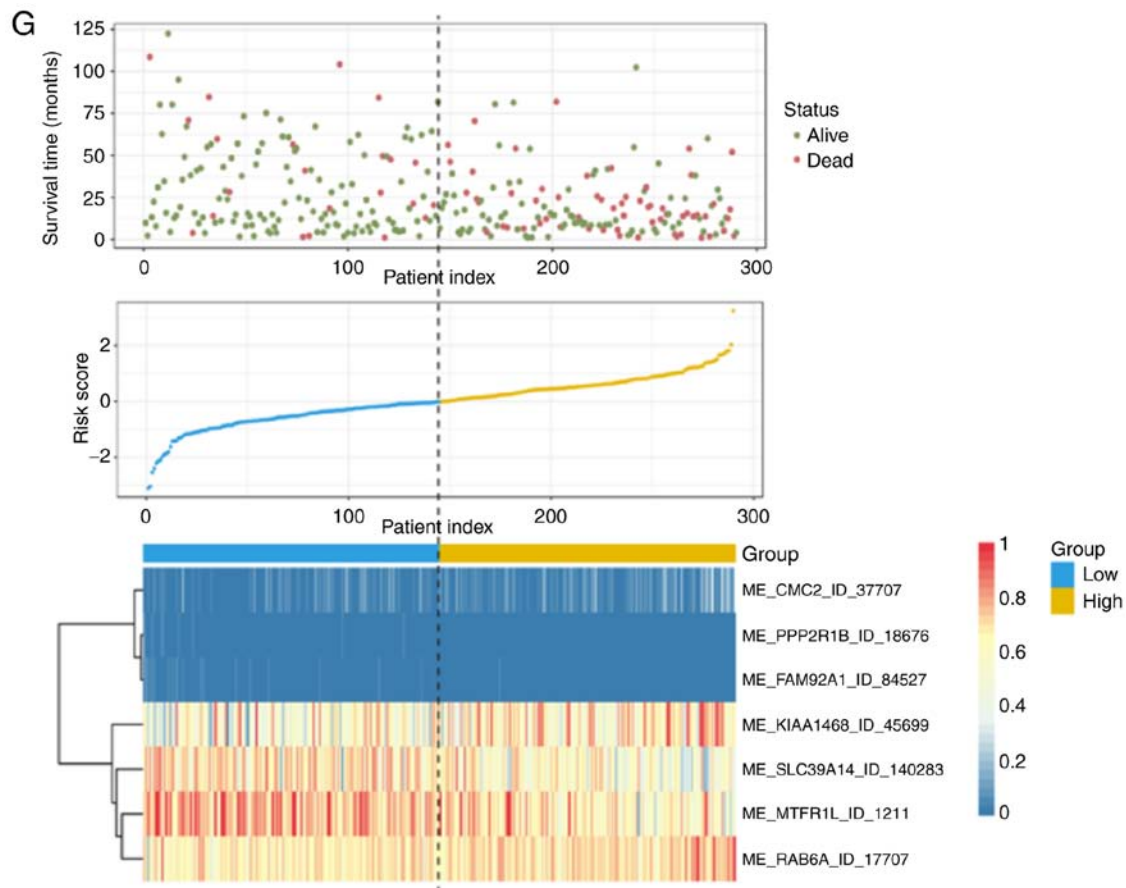
Figure 4. Continued. The color transition from blue to red indicates the increasing percent spliced in score of the corresponding AS event from low to high. For (G) ME, risk scores (corresponding to each AS type) were calculated and AS signatures were constructed using each type of prognostic splicing event. HCC, hepatocellular carcinoma; AS, alternative splicing; ES, exon skip; AT, alternate terminator; AP, alternate promoter; AA, alternate acceptor site; RI, retained intron; AD, alternate donor site; ME, mutually exclusive exons.

and inflammation (50). Similarly, KIA1 is regarded as a metastatic suppressor gene in HCC; in-depth investigation revealed that KITENIN, as a spliced variant of KAI1 lacking exon 7 at the COOH-terminal region, enhances distant metastasis by facilitating cell invasion and antagonizing the expression of KIA1 and other metastasis-suppressing genes (51). There has been much success in research into the diversity of HCC-specific splicing variants owning to the advancement of high-throughput technology. Hui *et al* analyzed eight paired tumor-normal HCC specimens using SMRT sequencing, and reported 233 novel AS events occurred in 223 known genes (52). More recently, Li *et al* identified 243 differential AS events in the development and progression of HCC, and these were closely involved in metabolism-related pathways and cancer hallmarks (53). Accordingly, aberrant AS events, considered as another hallmark of cancer, may serve as promising diagnostic, predictive and prognostic biomarkers for patients with HCC. However, due to the lack of corresponding clinical information and limited sample size, few have annotated the detected AS events with clinical meaning in a systematic manner, particularly for patients with HCC.

To the best of our knowledge, the present study is the first attempt at a comprehensive and integrated computational investigation of the AS event characteristics of HCC, further broadening the novel field of prognostic and molecule-targeted implications. Based on the splicing pattern and bioinformatics

algorithm of SpliceSeq, AS events can be roughly divided into seven types, which are depicted in Fig. 1C. Following strict filtering and screening, the preliminarily analysis detected a total of 34,163 AS events from 8,986 parent genes, among which the majority of detectable AS events belonged to the ES type (36.08%). Recently, the prognostic values of splicing variants have been widely identified in various types of cancer, including non-small cell lung cancer, pan-gastrointestinal adenocarcinomas, ovarian cancer and esophageal carcinoma (54-57). Such studies have developed a series of AS-based prognostic signatures that have performed fairly well in distinguishing between poor and good outcomes in relevant patients. Similarly, a total of 1,805 AS events from 1,314 parent genes were identified to be associated with OS in patients with HCC, using univariate Cox regression analyses. It is noteworthy that one gene can hold differential AS events that have a significantly opposite influence on survival according to the forest plots, which would have been undetectable if focus had been on transcriptional expression levels only, further highlighting the indispensable role of AS in oncogenesis. Compared with previous studies that used multivariate Cox regression analyses to screen key features in a prognostic panel, the present study applied the stepwise variable selection approach with the AIC criterion, which is more scientific and stringent for high-dimensional data mining. Encouragingly, the time-dependent ROC curves confirmed that the final AS signature, comprised of 26 AS events, had a
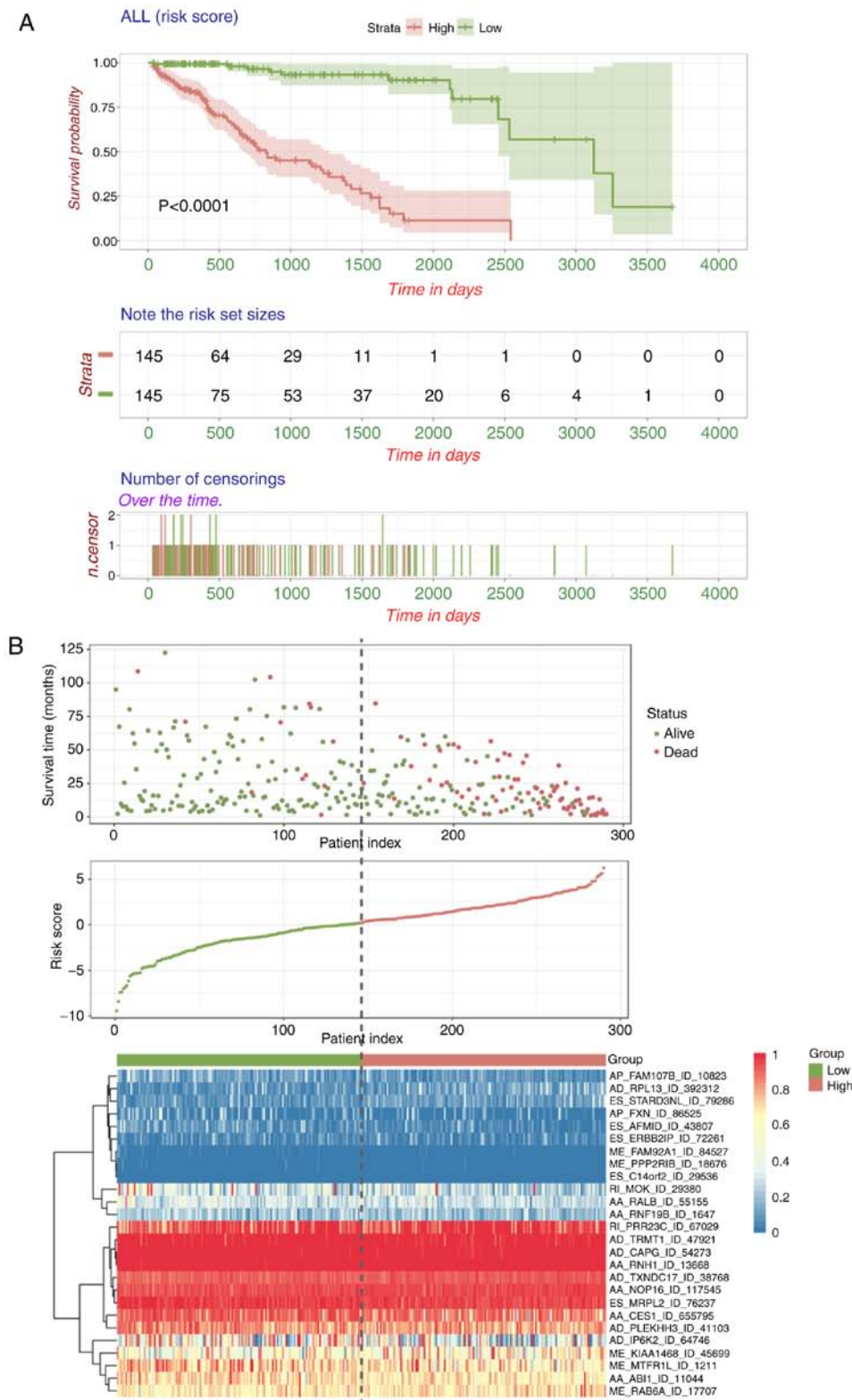
Figure 5. Construction and validation of final signature combining all types of prognostic AS event. (A) Kaplan-Meier curves of prognostic predictors built with all types of survival-associated splicing event. (B) Distribution of the survival status and risk scores of patients, and the splicing pattern of AS events included in the final AS signature. The color transition from blue to red indicates the increasing percent spliced in score of particular AS event from low to high. The colors of the ROC curves represent the different AS types and the respective AUC values are shown. HCC, hepatocellular carcinoma AS, alternative splicing; ROC, receiver-operator characteristic; AUC, area under the curve; ES, exon skip; AT, alternate terminator; AP, alternate promoter; AA, alternate acceptor site; RI, retained intron; AD, alternate donor site; ME, mutually exclusive exons.

noteworthy ability to distinguish between the distinct prognoses for patients with HCC, which also indicated that splicing events may be preeminent and ideal indicators for predicting cancer

prognoses. In addition, the proposed AS signature was independent of traditional clinical risk factors and of high clinical applicability in stratified patients.
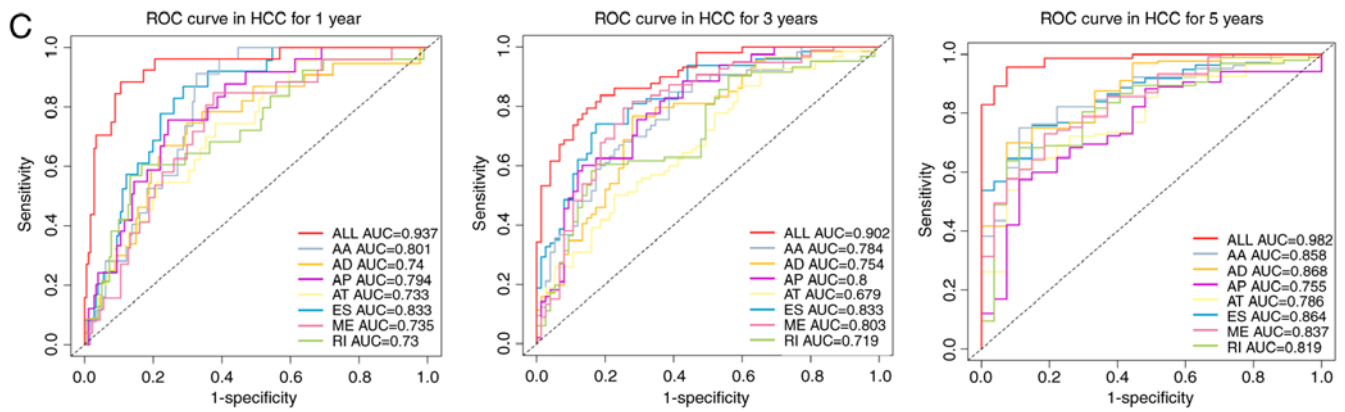
Figure 5. Continued. (C) ROC curves of all prognostic signatures for 1, 3 and 5 years in HCC. The colors of the ROC curves represent the different AS types and the respective AUC values are shown. HCC, hepatocellular carcinoma AS, alternative splicing; ROC, receiver-operator characteristic; AUC, area under the curve; ES, exon skip; AT, alternate terminator; AP, alternate promoter; AA, alternate acceptor site; RI, retained intron; AD, alternate donor site; ME, mutually exclusive exons.

Furthermore, the present study attempted to investigate the potential mechanism of prognostic AS events. Notably, the functional enrichment analysis revealed several significant interfered pathways, including ubiquitin-mediated proteolysis, ribosome and p53 signaling pathway, which were in accordance with previous studies concerning the genome-wide investigation of AS in gastrointestinal adenocarcinoma and colorectal cancer, respectively (40,56). Therefore, the cancer-related outcome resulting from AS alteration may be disturbed via certain shared cancer pathways. Additionally, it was revealed that the HIF-1 pathway and AMPK signaling pathway were significantly enriched biological processes, which have been gradually recognized to be associated with HCC-specific prognosis. For example, Jiang *et al* revealed that HIF-1 directly bound to the Rpn10 promoter and further promoted HCC cell proliferation (58). A cohort study (n=419) by Wang *et al* also suggested that HIF-1 was significantly associated with TNM stage, hepatitis B virus infection, tumor size, portal vein tumor thrombus and vascular invasion and further served as an independent adverse prognostic factor for patients with HCC with liver cirrhosis (59). AMP-activated protein kinase (AMPK), as a conserved heterotrimeric protein kinase complex, serves a vital role in cancer development and linking metabolism through mediating multiple mechanisms related to cell cycle, apoptosis and autophagy (60). *In vitro*, the phosphorylation status of AMPK has an anticancer effect via inhibition of the NF-κB signaling pathway in HCC (61). Previous investigations on HCC support the reliability and accuracy of the bioinformatics analyses performed in the present study. The results suggest that the poor outcomes of patients with HCC resulted from aberrant AS events that may be disturbed by a certain vital oncogenic biological process.

As widespread AS alterations within the tumor microenvironment may be extensively orchestrated by a limited number of SFs, the present study focused on the altered prognostic SFs and the SF-AS splicing correlation network. Through differential expression analysis combined with survival analysis, three SFs (SRSF10, PCBP2 and SFPQ) were filtered as candidates and all three were recognized as adverse prognostic factors. The function of splicing regulator SRSF10 may be partly mediated by the generation of BCLAF1-L through the alternative inclusion of exon 5a; the overexpression of the BCLAF1-L isoform has been shown to be associated with increased tumorigenic potential

and a higher tumor grade in colon cancer (62). Liu *et al* revealed that SRSF10 can modulate the AP events of IL-1 towards mIL1RAP in cervical cancer oncogenesis, which promoted NF-κB activation and inhibited macrophage phagocytosis (63). Poly(C)-binding protein 2 (PCBP2), as a multifunctional adapter that contributes to mRNA stabilization, translational silencing and enhancement via the poly(C)-binding motif, has been widely reported to mediate ambiguous functions in various types of cancer, including gastric cancer, breast cancer, pancreatic ductal adenocarcinoma, esophageal squamous cell carcinoma and glioblastoma (37,64-68). A particular AS event was also implicated in the presence of the binding site of PCBP2 within the exon 6 splicing acceptor (69). PCBP2 is pivotal in attenuating the innate immune response against hepatitis C infection and promoting alcoholic liver fibrosis, both of which are recognized as clinical carcinogenic factors for HCC (70,71). As a member of the *Drosophila* behavior Human Splicing family, SFPQ, containing both RNA- and DNA-binding motifs, is linked to multiple biological behaviors, including pre-mRNA splicing, transcriptional regulation and DNA mismatch repair (21,72,73). Previous studies have also revealed that SFPQ is correlated with the development of cisplatin resistance in liver cancer and regarded as an adverse prognostic biomarker (74). However, until now, few studies have addressed the involvement of SFs in AS events in HCC, and the regulatory roles of SFs in generating varied transcript isoforms require further validation in HCC samples. The splicing correlation network showed distinguished interactions between the identified SFs and the significant prognostic AS events. Of note, SFs can have opposite effects in the regulation of AS events, even from the same gene, and one particular AS event can be synergistically or antagonistically regulated by different SFs. This demonstrates that these complicated underlying connections offer potential clues to further understanding the crucial process that participates in regulation of HCC. Another noteworthy finding of the present study was that the majority of the favorable prognostic AS events were negatively regulated by SFs, whereas the risky AS events were mainly positively regulated by SFs. This indicates the multiple altered SFs may promote the invasive and metastatic potential of HCC via co-regulating the AS events of genes, which may offer novel insights for elucidating the mechanisms underlying the biogenesis and progression of HCC.

Table I. Detailed information of specific AS events involved in each AS signature and final prognostic model.

Gene symbol	AS ID	AS type	Exons	From exon	To exon	In final signature
ABI1	ID_11044	AA	11.1	9	11.2	Yes
SWI5	ID_87732	AA	3.1	2	3.2	No
CES1	ID_655795	AA	10.1	7	10.2	Yes
NOP16	ID_117545	AA	5.1	4.1	5.2	Yes
PPIL2	ID_61245	AA	22.4:22.5:22.6	22.2	22.7	No
RNH1	ID_13668	AA	6.1	5.3	6.2	Yes
HSD17B14	ID_50819	AA	4.1	3	4.2	No
RALB	ID_55155	AA	3.1	2	3.2	Yes
FXYD5	ID_49079	AA	1.5	1.1	1.6	No
RNF19B	ID_1647	AA	3.1	2	3.2	Yes
IP6K2	ID_64746	AD	11.6:11.7	11.5	11.9	Yes
TXNDC17	ID_38768	AD	1.2	1.1	2.1	Yes
RCHY1	ID_69521	AD	7.2	7.1	8.1	No
AURKAIP1	ID_152	AD	1.2	1.1	1.5	No
RPL13	ID_392312	AD	1.3:1.4	1.2	2	Yes
PLEKHH3	ID_41103	AD	11.2	11.1	12.2	Yes
CAPG	ID_54273	AD	7.2	7.1	8	Yes
TRMT1	ID_47921	AD	2.4	2.3	3	Yes
ATG9A	ID_57639	AD	10.2	10.1	11	No
ECI2	ID_75224	AD	1.2:1.3	1.1	2.1	No
MLST8	ID_33211	AP	2			No
GPR75-ASB3	ID_53555	AP				No
FAM107B	ID_10823	AP	4			Yes
FXN	ID_86525	AP	2			Yes
CLDN5	ID_61069	AP				No
TUBB3	ID_38167	AP	4			No
NFYC	ID_2015	AP	4			No
MTFR1L	ID_1211	ME	5|6	4.2	7.2	Yes
CMC2	ID_37707	ME	6|7	5	9	No
PPP2R1B	ID_18676	ME	4|5	3	6	Yes
SLC39A14	ID_140283	ME	5|6	4	7	No
RAB6A	ID_17707	ME	5|6	4	7	Yes
FAM92A1	ID_84527	ME	7|8	5.1	9.2	Yes
KIAA1468	ID_45699	ME	24|25	23	26	Yes
MOK	ID_29380	RI	15.2:15.3:15.4	15.1	15.5	Yes
MBD6	ID_22634	RI	13.4	13.3	13.5	No
C9orf9	ID_87994	RI	5.2	5.1	5.3	No
PSMC5	ID_43009	RI	2.2	2.1	2.3	No
NUDT22	ID_16589	RI	1.3	1.2	1.4	No
PRR23C	ID_67029	RI	1.2	1.1	1.3	Yes
HSF1	ID_85559	ES	10	9	11	No
MRPL2	ID_76237	ES	6	5	7	Yes
SNRPN	ID_29701	ES	11	10.4	12	No
SEC11A	ID_32314	ES	8	5	9	No
TPM3	ID_7792	ES	12	11	15	No
STARD3NL	ID_79286	ES	2	1	3	Yes
C14orf2	ID_29536	ES	3	2	5	Yes
ARHGEF1	ID_50101	ES	15	14	16	No
SFSWAP	ID_25214	ES	15	14	16.1	No
AFMID	ID_43807	ES	7:8:9:10	6	12	Yes
ERBB2IP	ID_72261	ES	22	21	24.1	Yes
PRRX1	ID_8968	AT	5			No

Table I. Continued.

Gene symbol	AS ID	AS type	Exons	From exon	To exon	In final signature
MASP1	ID_68075	AT	19			No
SLC4A4	ID_69463	AT	14.2			No
PLCH2	ID_273	AT	22.3			No
L3HYPDH	ID_27740	AT	7			No
AGAP1	ID_58086	AT	11			No

AS, alternative splicing; AA, alternate acceptor site; AD, alternate donor site; AP, alternate promoter; ME, mutually exclusive exons; RI, retained intron; ES, exon skip; AT, alternate terminator.
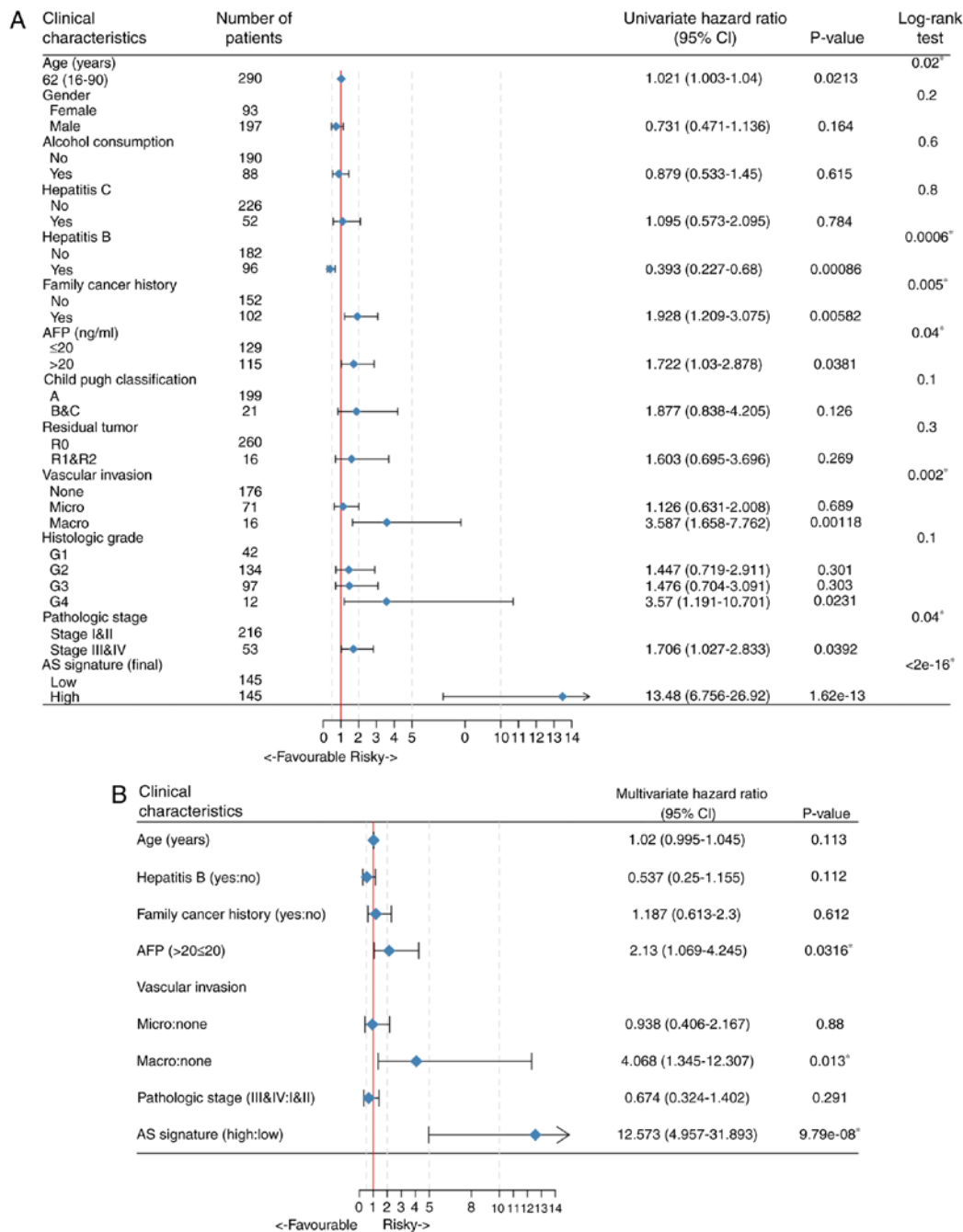

Figure 6. Forest plots of the associations of clinicopathological characteristics with OS in the hepatocellular carcinoma cohort. (A) Univariate Cox regression analysis of the relation between clinicopathological features and final AS signature regarding prognostic value. (B) Multivariate Cox analysis of the associations between clinical risk factors, including age, hepatitis B, family cancer history, AFP level, vascular invasion, pathologic stage and AS signature, and OS. The hazard ratios (blue diamonds) and 95% CI (horizontal lines) are depicted, respectively. AS, alternative splicing; OS, overall survival; CI, confidence intervals; AFP, α-fetoprotein.
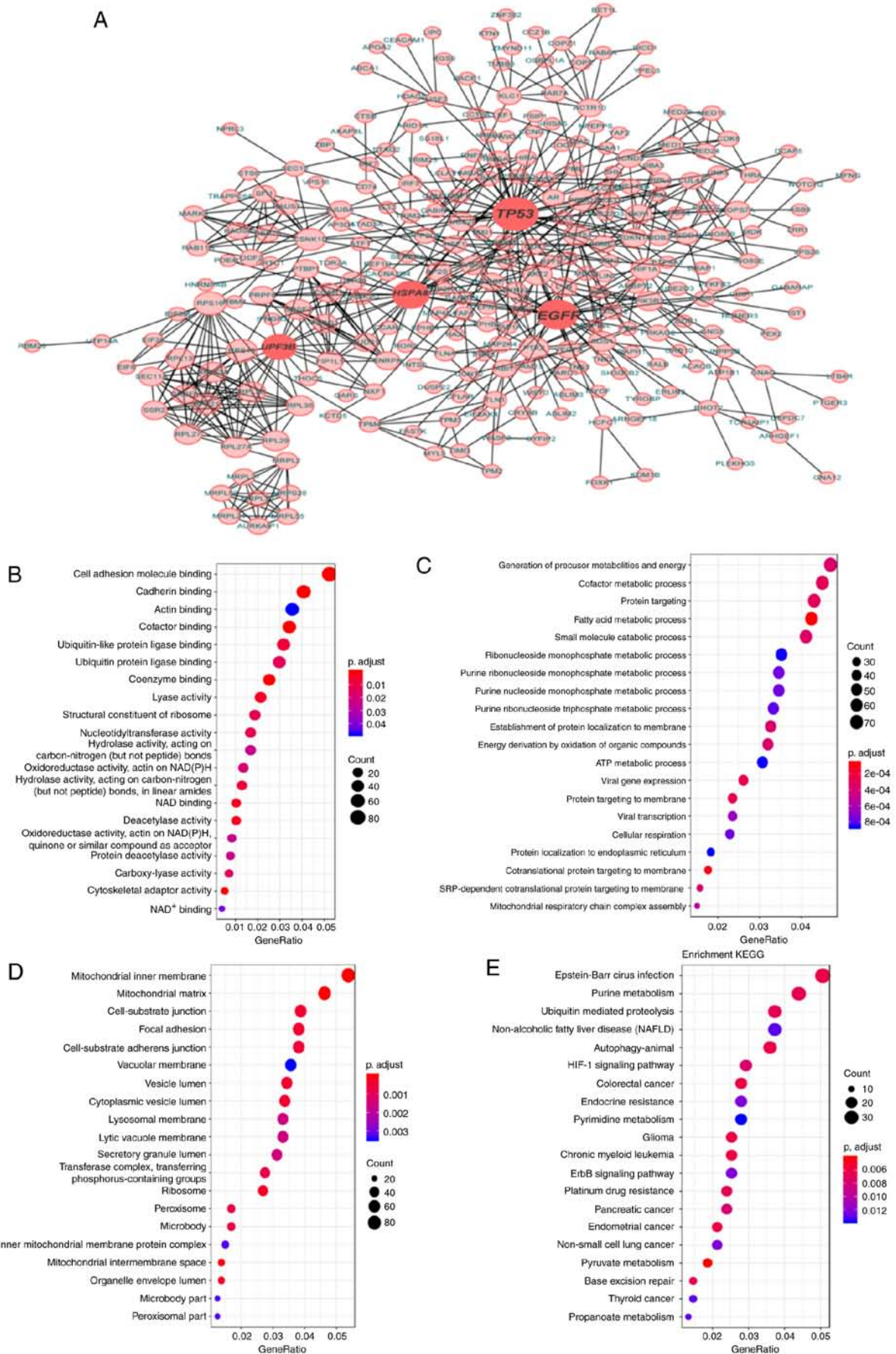
Figure 7. Gene interaction network and functional enrichment analysis for prognosis-related AS events in HCC. (A) Gene interaction network of survival-associated AS events in HCC. Top 20 Gene Ontology terms in (B) molecular function, (C) biological process and (D) cellular component. (E) Top 20 significantly enriched KEGG pathways. The size and color of nodes represents the enriched gene number and false discovery rate, respectively. HCC, hepatocellular carcinoma; AS, alternative splicing; KEGG, Kyoto Encyclopedia of Genes and Genomes.
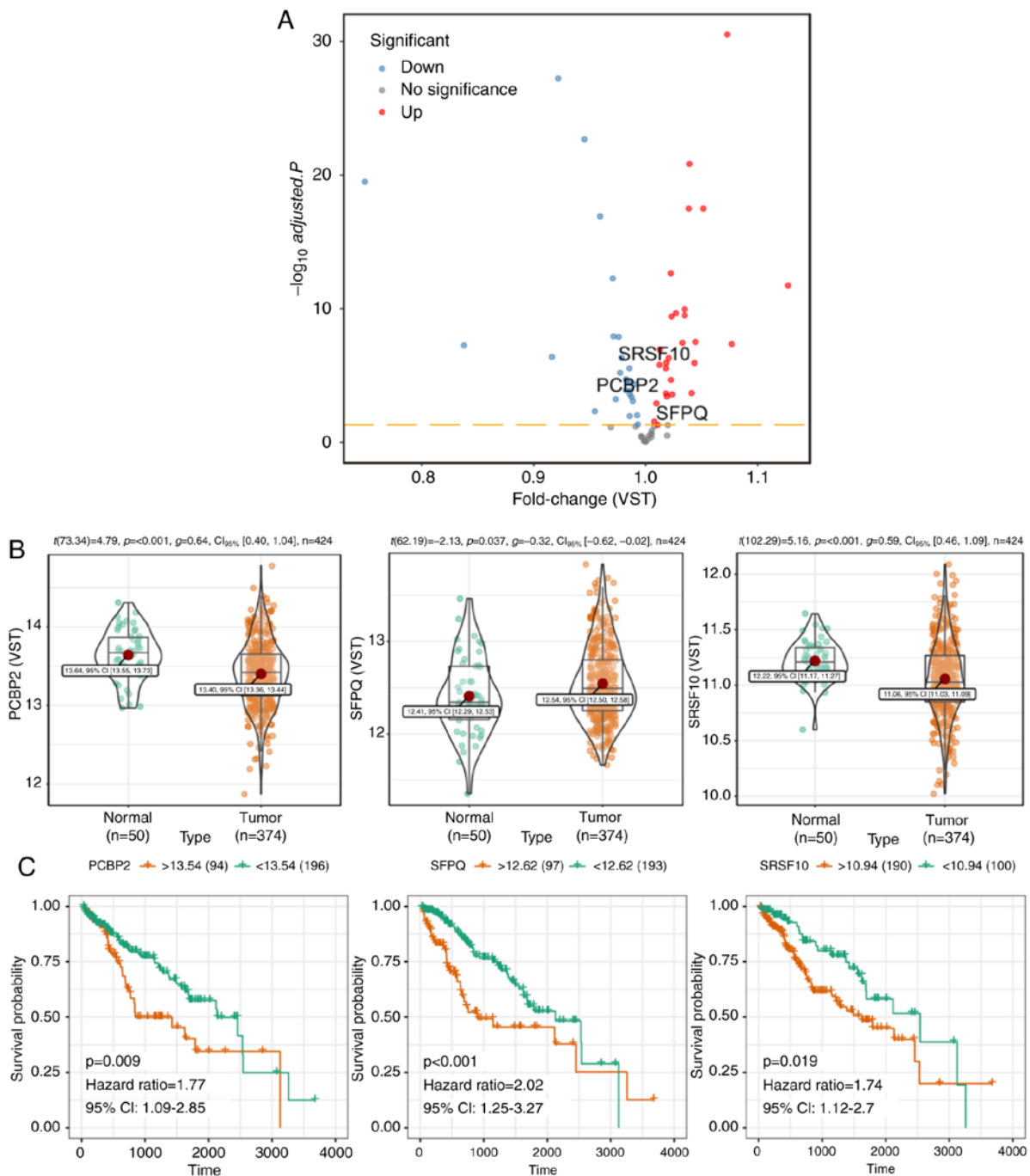
Figure 8. Construction of a potential SF-AS regulatory network in HCC. (A) Volcano plot visualizing differential expressed SFs in The Cancer Genome Atlas dataset of HCC. The red and blue dots in the plot represent the differentially expressed SFs with statistical significance (adjusted P<0.05). And the prognostic SFs are marked in the diagram. (B) Relative expression levels (VST) of screened prognostic SFs (PCBP2, SFPQ and SRSF10) between primary HCC and para-cancerous tissues. (C) Kaplan-Meier survival curves of PCBP2, SFPQ and SRSF10 in the HCC cohort with optimal cut-off values shown. HCC, hepatocellular carcinoma; AS, alternative splicing; SF, splicing factor; VST, variance stabilizing transformation; PSI, percent spliced in; CI, confidence intervals; RI, retained intron; AD, alternate donor site; ES, exon skip; AT, alternate terminator.

However, there were several limitations in the present study that require clarification. Firstly, the patients enrolled were exclusively from a single cohort and the sample size of the HCC cohort was limited. Secondly, due to the lack of other independent cohort concerning AS events among HCC patients, further validation and reproducible analysis could not be performed at present. Thirdly, owing to the retrospective nature of the present study, prospective cohorts with a larger sample size are warranted. Therefore, further verification of the *in silico* analysis performed is required in the future.

In conclusion, the present study provided a comprehensive picture of the global changes in mRNA splicing signatures in HCC, developed a robust prognostic model and constructed a splicing correlation network, were valuable in elucidating the underlying mechanisms of AS and contributed to the identification of novel prognostic markers and therapeutic targets for further validation.
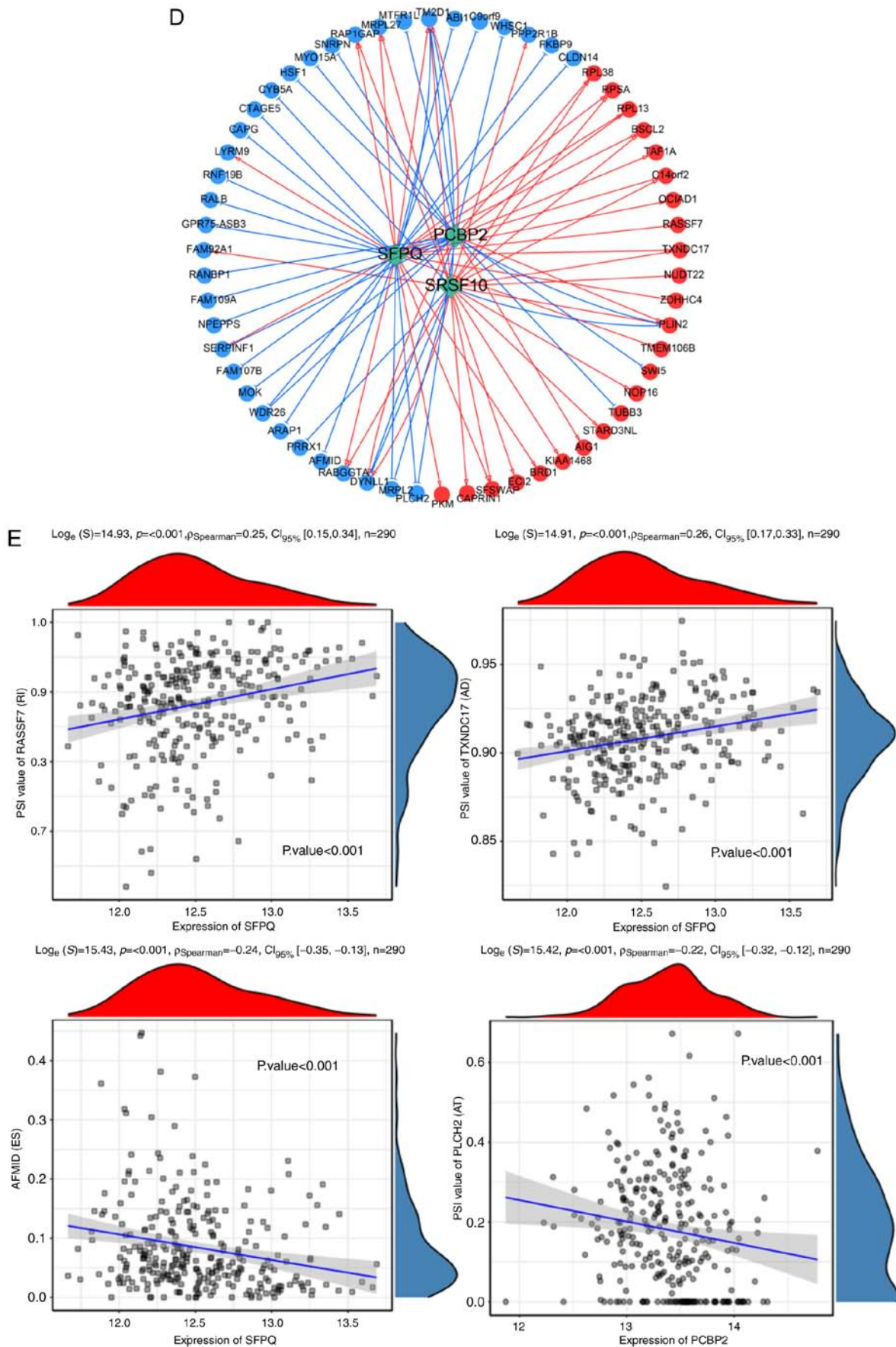
Figure 8. Continued. (D) Splicing correlation network built among the significant correlation pairs. Three prognostic SFs (green diamonds) were positively (red line) or negatively (blue line) correlated with 36 favorable AS events (blue dots) and 26 adverse AS events (red dots). (E) Representative scatter plots between the normalized expression (VST) of the particular SF and PSI score of the AS event. HCC, hepatocellular carcinoma; AS, alternative splicing; SF, splicing factor; VST, variance stabilizing transformation; PSI, percent spliced in; CI, confidence intervals; RI, retained intron; AD, alternate donor site; ES, exon skip; AT, alternate terminator.

Availability of data and materials

The RNA-seq data, splicing variant data and clinical information of HCC used in this study were acquired and integrated from the TCGA and TCGA SpliceSeq.

Authors' contributions

DZ and JL contributed to the conception and design of the study. YD and ZW also participated in the conception of the study. DZ performed the statistical analysis. DZ and YD were involved in the preparation of the figures and tables. DZ, ZW and YD reviewed the results and participated in the discussion of the data. DZ and YD prepared and wrote the manuscript. ZW and JL revised the manuscript. All authors read and approved the final version of this manuscript.

Ethics approval and consent to participate

Not applicable.

Patient consent for publication

Not applicable.

Competing interests

The authors declare that they have no competing interests.

References

1. Ferlay J, Soerjomataram I, Dikshit R, Eser S, Mathers C, Rebelo M, Parkin DM, Forman D and Bray F: Cancer incidence and mortality worldwide: Sources, methods and major patterns in GLOBOCAN 2012. Int J Cancer 136: E359-E386, 2015.
2. Vitale A, Peck-Radosavljevic M, Giannini EG, Vibert E, Sieghart W, Van Poucke S and Pawlik TM: Personalized treatment of patients with very early hepatocellular carcinoma. J Hepatol 66: 412-423, 2017.
3. Ulahannan SV, Duffy AG, McNeel TS, Kish JK, Dickie LA, Rahma OE, McGlynn KA, Greten TF and Altekruse SF: Earlier presentation and application of curative treatments in hepatocellular carcinoma. Hepatology 60: 1637-1644, 2014.
4. Tabrizian P, Jibara G, Shrager B, Schwartz M and Roayaie S: Recurrence of hepatocellular cancer after resection: Patterns, treatments, and prognosis. Ann Surg 261: 947-955, 2015.
5. Wang JH, Wang CC, Hung CH, Chen CL and Lu SN: Survival comparison between surgical resection and radiofrequency ablation for patients in BCLC very early/early stage hepatocellular carcinoma. J Hepatol 56: 412-418, 2012.
6. Ueno M, Hayami S, Shigekawa Y, Kawai M, Hirono S, Okada K, Tamai H, Shingaki N, Mori Y, Ichinose M and Yamaue H: Prognostic impact of surgery and radiofrequency ablation on single nodular HCC 5 cm: Cohort study based on serum HCC markers. J Hepatol 63: 1352-1359, 2015.
7. Hiraoka A, Kumada T, Kudo M, Hirooka M, Tsuji K, Itobayashi E, Kariyama K, Ishikawa T, Tajiri K, Ochi H, *et al*: Albumin-bilirubin (ALBI) grade as part of the evidence-based clinical practice guideline for HCC of the japan society of hepatology: A comparison with the liver damage and child-pugh classifications. Liver Cancer 6: 204-215, 2017.
8. Li S and Mao M: Next generation sequencing reveals genetic landscape of hepatocellular carcinomas. Cancer Lett 340: 247-253, 2013.
9. Huang W, Skanderup AJ and Lee CG: Advances in genomic hepatocellular carcinoma research. Gigascience 7: 11, 2018.
10. Zhang YC, Zhou Q and Wu YL: The emerging roles of NGS-based liquid biopsy in non-small cell lung cancer. J Hematol Oncol 10: 167, 2017.
11. Cancer Genome Atlas Research Network. Electronic address: wheeler@bcm.edu; Cancer Genome Atlas Research Network: Comprehensive and integrative genomic characterization of hepatocellular carcinoma. Cell 169: 1327-1341.e23, 2017.
12. Villanueva A, Portela A, Sayols S, Battiston C, Hoshida Y, Mendez-Gonzalez J, Imbeaud S, Letouzé E, Hernandez-Gea V, Cornella H, *et al*: DNA methylation-based prognosis and epidrivers in hepatocellular carcinoma. Hepatology 61: 1945-1956, 2015.
13. Qiu J, Peng B, Tang Y, Qian Y, Guo P, Li M, Luo J, Chen B, Tang H, Lu C, *et al*: CpG Methylation signature predicts recurrence in early-stage hepatocellular carcinoma: Results from a multicenter study. J Clin Oncol 35: 734-742, 2017.
14. Long J, Wang A, Bai Y, Lin J, Yang X, Wang D, Yang X, Jiang Y and Zhao H: Development and validation of a TP53-associated immune prognostic model for hepatocellular carcinoma. EBioMedicine 42: 363-374, 2019.
15. Long J, Bai Y, Yang X, Lin J, Yang X, Wang D, He L, Zheng Y and Zhao H: Construction and comprehensive analysis of a ceRNA network to reveal potential prognostic biomarkers for hepatocellular carcinoma. Cancer Cell Int 19: 90, 2019.
16. Baralle FE and Giudice J: Alternative splicing as a regulator of development and tissue identity. Nat Rev Mol Cell Biol 18: 437-451, 2017.
17. Gamazon ER and Stranger BE: Genomics of alternative splicing: Evolution, development and pathophysiology. Hum Genet 133: 679-687, 2014.
18. Wang ET, Sandberg R, Luo S, Khrebtukova I, Zhang L, Mayr C, Kingsmore SF, Schroth GP and Burge CB: Alternative isoform regulation in human tissue transcriptomes. Nature 456: 470-476, 2008.
19. Montes M, Sanford BL, Comiskey DF and Chandler DS: RNA Splicing and disease: Animal models to therapies. Trends Genet 35: 68-87, 2019.
20. Climente-Gonzalez H, Porta-Pardo E, Godzik A and Eyras E: The functional impact of alternative splicing in cancer. Cell Rep 20: 2215-2226, 2017.
21. Tao Y, Ma C, Fan Q, Wang Y, Han T and Sun C: MicroRNA-1296 facilitates proliferation, migration and invasion of colorectal cancer cells by targeting SFPQ. J Cancer 9: 2317-2326, 2018.
22. David CJ and Manley JL: Alternative pre-mRNA splicing regulation in cancer: Pathways and programs unhinged. Genes Dev 24: 2343-2364, 2010.
23. Song X, Zeng Z, Wei H and Wang Z: Alternative splicing in cancers: From aberrant regulation to new therapeutics. Semin Cell Dev Biol 75: 13-22, 2018.
24. Lu Y, Xu W, Ji J, Feng D, Sourbier C, Yang Y, Qu J, Zeng Z, Wang C, Chang X, *et al*: Alternative splicing of the cell fate determinant numb in hepatocellular carcinoma. Hepatology 62: 1122-1131, 2015.
25. Berasain C, Goni S, Castillo J, Latasa MU, Prieto J and Avila MA: Impairment of pre-mRNA splicing in liver disease: Mechanisms and consequences. World J Gastroenterol 16: 3091-3102, 2010.
26. Ratnadiwakara M, Mohenska M and Anko ML: Splicing factors as regulators of miRNA biogenesis-links to human disease. Semin Cell Dev Biol 79: 113-122, 2018.
27. Chen M and Manley JL: Mechanisms of alternative splicing regulation: Insights from molecular and genomics approaches. Nat Rev Mol Cell Biol 10: 741-754, 2009.
28. Wahl MC, Will CL and Luhrmann R: The spliceosome: Design principles of a dynamic RNP machine. Cell 136: 701-718, 2009.
29. Prochazka L, Tesarik R and Turanek J: Regulation of alternative splicing of CD44 in cancer. Cell Signal 26: 2234-2239, 2014.
30. Yoshida K and Ogawa S: Splicing factor mutations and cancer. Wiley Interdiscip Rev RNA 5: 445-459, 2014.

31. El Marabti E and Younis I: The cancer spliceome: Reprograming of alternative splicing in cancer. Front Mol Biosci 5: 80, 2018.
32. Anczukow O and Krainer AR: Splicing-factor alterations in cancers. RNA 22: 1285-1301, 2016.
33. Tomczak K, Czerwinska P and Wiznerowicz M: The cancer genome atlas (TCGA): An immeasurable source of knowledge. Contemp Oncol (Pozn) 19: A68-A77, 2015.
34. Ryan MC, Cleland J, Kim R, Wong WC and Weinstein JN: SpliceSeq: A resource for analysis and visualization of RNA-Seq data on alternative splicing and its functional impacts. Bioinformatics 28: 2385-2387, 2012.
35. Liao SG, Lin Y, Kang DD, Chandra D, Bon J, Kaminski N, Sciurba FC and Tseng GC: Missing value imputation in high-dimensional phenomic data: Imputable or not, and how? BMC Bioinformatics 15: 346, 2014.
36. Lex A, Gehlenborg N, Strobelt H, Vuillemot R and Pfister H: UpSet: Visualization of intersecting sets. IEEE Trans Vis Comput Graph 20: 1983-1992, 2014.
37. Ye J, Zhou G, Zhang Z, Sun L, He X and Zhou J: Poly (C)-binding protein 2 (PCBP2) promotes the progression of esophageal squamous cell carcinoma (ESCC) through regulating cellular proliferation and apoptosis. Pathol Res Pract 212: 717-725, 2016.
38. Kamarudin AN, Cox T and Kolamunnage-Dona R: Time-dependent ROC curve analysis in medical research: Current methods and applications. BMC Med Res Methodol 17: 53, 2017.
39. Yu G, Wang LG, Han Y and He QY: ClusterProfiler: An R package for comparing biological themes among gene clusters. OMICS 16: 284-287, 2012.
40. Xiong Y, Deng Y, Wang K, Zhou H, Zheng X, Si L and Fu Z: Profiles of alternative splicing in colorectal cancer and their clinical significance: A study based on large-scale sequencing data. EBioMedicine 36: 183-195, 2018.
41. Piva F, Giulietti M, Burini AB and Principato G: SpliceAid 2: A database of human splicing factors expression data and RNA target motifs. Hum Mutat 33: 81-85, 2012.
42. Love MI, Huber W and Anders S: Moderated estimation of fold change and dispersion for RNA-seq data with DESeq2. Genome Biol 15: 550, 2014.
43. Hänzelmann S, Castelo R and Guinney J: GSVA: Gene set variation analysis for microarray and RNA-Seq data. BMC Bioinformatics 14: 7, 2013.
44. Ritchie ME, Phipson B, Wu D, Hu Y, Law CW, Shi W and Smyth GK: Limma powers differential expression analyses for RNA-sequencing and microarray studies. Nucleic Acids Res 43: e47, 2015.
45. Lin DC, Mayakonda A, Dinh HQ, Huang P, Lin L, Liu X, Ding LW, Wang J, Berman BP, Song EW, et al: Genomic and epigenomic heterogeneity of hepatocellular carcinoma. Cancer Res 77: 2255-2265, 2017.
46. Wang BD and Lee NH: Aberrant RNA splicing in cancer and drug resistance. Cancers (Basel) 10: 11, 2018.
47. Shi YM, Li YY, Lin JY, Zheng L, Zhu YM and Huang J: The discovery of a novel eight-mRNA-lncRNA signature predicting survival of hepatocellular carcinoma patients. J Cell Biochem: Nov 28, 2018 (Epub ahead of print). doi: 10.1002/jcb.28028.
48. Liu G, Wang H, Fu JD, Liu JY, Yan AG and Guan YY: A five-miRNA expression signature predicts survival in hepatocellular carcinoma. APMIS 125: 614-622, 2017.
49. Gu JX, Zhang X, Miao RC, Xiang XH, Fu YN, Zhang JY, Zhang JY, Liu C and Qu K: Six-long non-coding RNA signature predicts recurrence-free survival in hepatocellular carcinoma. World J Gastroenterol 25: 220-232, 2019.
50. Dayton TL, Gocheva V, Miller KM, Israelsen WJ, Bhutkar A, Clish CB, Davidson SM, Luengo A, Bronson RT, Jacks T and Vander Heiden MG: Germline loss of PKM2 promotes metabolic distress and hepatocellular carcinoma. Genes Dev 30: 1020-1033, 2016.
51. Lee JH, Park SR, Chay KO, Seo YW, Kook H, Ahn KY, Kim YJ and Kim KK: KAI1 COOH-terminal interacting tetraspanin (KITENIN), a member of the tetraspanin family, interacts with KAI1, a tumor metastasis suppressor, and enhances metastasis of cancer. Cancer Res 64: 4235-4243, 2004.
52. Chen H, Gao F, He M, Ding XF, Wong AM, Sze SC, Yu AC, Sun T, Chan AW, Wang X and Wong N: Long-read RNA sequencing identifies Alternative splice variants in hepatocellular carcinoma and tumor-specific isoforms. Hepatology: Jan 13, 2019 (Epub ahead of print). doi: 10.1002/hep.30500.
53. Li S, Hu Z, Zhao Y, Huang S and He X: Transcriptome-wide analysis reveals the landscape of aberrant alternative splicing events in liver cancer. Hepatology 69: 359-375, 2019.

54. Li Y, Sun N, Lu Z, Sun S, Huang J, Chen Z and He J: Prognostic alternative mRNA splicing signature in non-small cell lung cancer. Cancer Lett 393: 40-51, 2017.
55. Zhu J, Chen Z and Yong L: Systematic profiling of alternative splicing signature reveals prognostic predictor for ovarian cancer. Gynecol Oncol 148: 368-374, 2018.
56. Lin P, He RQ, Ma FC, Liang L, He Y, Yang H, Dang YW and Chen G: Systematic analysis of survival-associated alternative splicing signatures in gastrointestinal pan-adenocarcinomas. EBioMedicine 34: 46-60, 2018.
57. Mao S, Li Y, Lu Z, Che Y, Sun S, Huang J, Lei Y, Wang X, Liu C, Zheng S, et al: Survival-associated alternative splicing signatures in esophageal carcinoma. Carcinogenesis 40: 121-130, 2019.
58. Jiang Z, Zhou Q, Ge C, Yang J, Li H, Chen T, Xie H, Cui Y, Shao M, Li J and Tian H: Rpn10 promotes tumor progression by regulating hypoxia-inducible factor 1 alpha through the PTEN/Akt signaling pathway in hepatocellular carcinoma. Cancer Lett 447: 1-11, 2019.
59. Wang D, Zhang X, Lu Y, Wang X and Zhu L: Hypoxia inducible factor 1α in hepatocellular carcinoma with cirrhosis: Association with prognosis. Pathol Res Pract 214: 1987-1992, 2018.
60. Jones RG and Thompson CB: Tumor suppressors and cell metabolism: A recipe for cancer growth. Genes Dev 23: 537-548, 2009.
61. Zheng L, Yang W, Wu F, Wang C, Yu L, Tang L, Qiu B, Li Y, Guo L, Wu M, et al: Prognostic significance of AMPK activation and therapeutic effects of metformin in hepatocellular carcinoma. Clin Cancer Res 19: 5372-5380, 2013.
62. Zhou X, Li X, Cheng Y, Wu W, Xie Z, Xi Q, Han J, Wu G, Fang J and Feng Y: BCLAF1 and its splicing regulator SRSF10 regulate the tumorigenic potential of colon cancer cells. Nat Commun 5: 4581, 2014.
63. Liu F, Dai M, Xu Q, Zhu X, Zhou Y, Jiang S, Wang Y, Ai Z, Ma L, Zhang Y, et al: SRSF10-mediated IL1RAP alternative splicing regulates cervical cancer oncogenesis via mIL1RAP-NF-κB-CD47 axis. Oncogene 37: 2394-2409, 2018.
64. Chen C, Lei J, Zheng Q, Tan S, Ding K and Yu C: Poly(rC) binding protein 2 (PCBP2) promotes the viability of human gastric cancer cells by regulating CDK2. FEBS Open Bio 8: 764-773, 2018.
65. Luo K and Zhuang K: High expression of PCBP2 is associated with progression and poor prognosis in patients with glioblastoma. Biomed Pharmacother 94: 659-665, 2017.
66. Li F, Bullough KZ, Vashisht AA, Wohlschlegel JA and Philpott CC: Poly(rC)-binding protein 2 regulates hippo signaling to control growth in breast epithelial cells. Mol Cell Biol 36: 2121-2131, 2016.
67. Hu CE, Liu YC, Zhang HD and Huang GJ: The RNA-binding protein PCBP2 facilitates gastric carcinoma growth by targeting miR-34a. Biochem Biophys Res Commun 448: 437-442, 2014.
68. Wan C, Gong C, Zhang H, Hua L, Li X, Chen X, Chen Y, Ding X, He S, Cao W, et al: β2-adrenergic receptor signaling promotes pancreatic ductal adenocarcinoma (PDAC) progression through facilitating PCBP2-dependent c-myc expression. Cancer Lett 373: 67-76, 2016.
69. Ghanem LR, Kromer A, Silverman IM, Ji X, Gazzara M, Nguyen N, Aguilar G, Martinelli M, Barash Y and Liebhaber SA: Poly(C)-binding protein Pcbp2 enables differentiation of definitive erythropoiesis by directing functional splicing of the runx1 transcript. Mol Cell Biol 38: 16, 2018.
70. Liu H, Chen Z, Jin W, Barve A, Wan YY and Cheng K: Silencing of α-complex protein-2 reverses alcohol- and cytokine-induced fibrogenesis in hepatic stellate cells. Liver Res 1: 70-79, 2017.
71. Qin Y, Xue B, Liu C, Wang X, Tian R, Xie Q, Guo M, Li G, Yang D and Zhu H: NLRX1 mediates MAVS degradation to attenuate the hepatitis C virus-induced innate immune response through PCBP2. J Virol 91: 23, 2017.
72. Mora Gallardo C, Sánchez de Diego A, Gutiérrez Hernández J, Talavera-Gutiérrez A, Fischer T, Martínez-A C and van Wely KHM: Dido3-dependent SFPQ recruitment maintains efficiency in mammalian alternative splicing. Nucleic Acids Res 47: 5381-5394, 2019.
73. Ray D, Kazan H, Cook KB, Weirauch MT, Najafabadi HS, Li X, Gueroussov S, Albu M, Zheng H, Yang A, et al: A compendium of RNA-binding motifs for decoding gene regulation. Nature 499: 172-177, 2013.
74. Ru Y, Chen XJ, Guo WZ, Gao SG, Qi YJ, Chen P, Feng XS and Zhang SJ: NEAT1_2-SFPQ axis mediates cisplatin resistance in liver cancer cells in vitro. Onco Targets Ther 11: 5695-5702, 2018.